PRODUCTION OF BORON NITRIDE USING CHEMICAL VAPOR DEPOSITION METHOD

A THESIS SUBMITTED TO
THE GRADUATE SCHOOL OF NATURE AND APPLIED SCIENCES
OF
MIDDLE EAST TECHNICAL UNIVERSITY

BY

ÖZGE MERCAN

IN PARTIAL FULFILLMENT OF THE REQUIREMENTS
FOR
THE DEGREE OF MASTER OF SCIENCE
IN
CHEMICAL ENGINEERING

FEBRUARY 2014

Approval of the thesis:

PRODUCTION OF BORON NITRIDE USING CHEMICAL VAPOR DEPOSITION METHOD

submitted by **ÖZGE MERCAN** in partial fulfillment of the requirements for the degree of **Master of Science in Chemical Engineering Department, Middle East Technical University** by,

Prof. Dr. Canan Özgen
Dean, Graduate School of **Natural and Applied Sciences** _____

Prof. Dr. Halil Kalıpçılar
Head of Department, **Chemical Engineering,** _____

Prof. Dr. H. Önder Özbelge
Supervisor, **Chemical Engineering Dept,** _____

Assoc. Prof. Dr. Naime Aslı Sezgi
Co-supervisor, **Chemical Engineering Dept,** _____

Examining Committee Members

Prof. Dr. Hayrettin Yücel _____
Chemical Engineering Department, METU

Prof. Dr. H. Önder Özbelge _____
Chemical Engineering Department, METU

Prof. Dr. Nail Yaşyerli _____
Chemical Engineering Department, Gazi Unv.

Prof. Dr. Halil Kalıpçılar _____
Chemical Engineering Department, METU

Yard. Doç. Dr. Zeynep Çulfaz Emecen _____
Chemical Engineering Department, METU

Date : _____

I hereby declare that all information in this document has been obtained and presented in accordance with academic rules, and ethical conduct. I also declare that, as required by these rules and conduct, I have fully cited and referenced all material and results that are not original to this work.

Name, Last Name : ÖZGE MERCAN

Signature :

ABSTRACT

PRODUCTION OF BORON NITRIDE USING CHEMICAL VAPOR DEPOSITION METHOD

Mercan, Özge

Master of Science, Department of Chemical Engineering

Supervisor : Prof. Dr. H. Önder Özbelge

Co-Supervisor: Assoc. Prof. Dr. N. Aslı Sezgi

February 2013, 77 pages

Boron nitride is a promising material with its outstanding characteristics like chemical inertness, large band gap, high oxidation resistance and thermal conductivity. It is also used as ceramic matrix component which transfers external load and deflects matrix cracks. Therefore, it has become a subject matter for many studies.

In this study, the process of boron nitride (BN) production from diborane (B_2H_6) and ammonia (NH_3) on tungsten (W) substrate in impinging jet reactor is investigated using chemical vapor deposition (CVD) method. The process parameters; temperature of the substrate, total gas flow rate and concentration ratio of the precursors are studied to obtain the highest deposition rate in the impinging jet reactor. The composition, structure and morphology of the produced films were studied using XRD, XPS, Raman Spectroscopy and SEM methods. XRD analyses of the products showed that boron nitride formed on the tungsten substrate. Atomic ratio of the elements in the produced film was obtained from XPS analysis which shows that other boron products might be

formed in the product as well. Raman Spectroscopy gave information about the existence of the B-N bonds. SEM analyses showed that the morphology of the produced films changes with respect to temperature.

Effect of temperature on deposition rate was studied between 900^{o}C and 1200^{o}C. It is found that deposition rate is positively correlated with temperature. Different molar ratios of B_2H_6 to NH_3 were studied in order to analyze the effects of different molar ratios on the deposition rate and morphology of the film. It is found that, at the molar ratio of 0.033 and 0.099, the morphology of the film is similar. At the molar ratio of 0.050, rounded grains on the topography were observed. Deposition rate of the film reaches to maximum when the reactants are fed to the reactor at the molar ratio of 0.050. The effects of total flow rate on the deposited film were investigated keeping the concentration of the reactants constant. Total flow rate is negatively correlated with deposition rate due to the residence time of the reactants in the reactor. Thickness analyses were done to observe the profile throughout the film. As a result, it is found that the highest deposition rate is obtained at the temperature of 1200^{o}C with a total flow rate of 150 ml/min and molar ratio ($[B_2H_6]/[NH_3]$) of 0.050.

Keywords: CVD, Boron Nitride, BN, Tungsten

ÖZ

KİMYASAL BUHAR BİRİKTİRME METHODU KULLANARAK BOR NİTRÜR ÜRETİMİ

Mercan, Özge
Yüksek lisans, Kimya Mühendisliği Bölümü
Tez Yöneticisi : Prof. Dr. H. Önder Özbelge
Ortak Tez Yöneticisi: Assoc. Prof. Dr. Naime A. Sezgi

Şubat 2014, 77 sayfa

Bor nitrür, kimyasal inertlik, geniş band açıklığı, yüksek oksitlenme direnci ve ısı iletkenliği gibi üstün özellileri ile gelecek vaat eden bir malzemedir. Ayrıca, seramik matriks bileşeni olarak dış yükü dağıtmada ve matriks çatlaklarının yönünü değiştirmede de kullanılmaktadır. Bu nedenle, birçok çalışmanın konu başlığı olmuştur.

Bu çalışma, kimyasal buhar biriktirme yöntemi (CVD) kullanılarak çift taraflı çarpan jet reaktörde diboran (B_2H_6) ve amonyak (NH_3) gazlarından, tungsten (W) üzerine biriktirilen bor nitrür (BN) üretimini incelemektedir. Yüzey sıcaklığı, toplam gaz akışı ve reaktant gazların konsantrasyon oranı gibi üretim parametreleri tartışılarak çarpan jet reaktöründeki BN üretimi çalışılmıştır. XPS, XRD, Raman Spectrum ve SEM analizleri kullanılarak üretilen bor nitrür (BN) ince filminin karakterizasyonu yapılıp, yapısı ve morfolojisi incelenmiştir. XRD analizi, bor nitrürün tungsten yüzey üzerinde oluştuğunu göstermiştir. Üretilen filmdeki elementlerin atomik oranları XPS analizi ile elde edilmiştir buna gore ürün içerisinde bor nitrür dışında başka borlu birleşikler olabileceği ortaya çıkmıştır. Raman spectroscopy üretilen film içerisindeki B-N bağlarının varlığı ile

ilgili bilgi vermiştir. SEM analizi göstermiştir ki üretilen filmin morfolojisi sıcaklık ile değişmektedir.

Sıcaklığın biriktirme hızına etkisi 900^{o}C – 1200^{o}C sıcaklık aralığında çalışılmıştır. Biriktirme hızının sıcaklık ile doğru orantılı olarak arttığı bulunmuştur. Toplam gaz akışındaki farklı diboran ve amonyak molar oranlarının biriktirme hızına ve üretilen filmin morfolojisine olan etkileri çalışılmıştır. Film boyunca oluşan profili gözlemlemek için kalınlık analizi yapılmıştır. Buna göre, film biriktirme hızı reaktantlar reaktöre 0.050 molar oranda ($[B_2H_6]/[NH_3]$) beslendiğinde maksimuma ulaşmaktadır. Toplam akış hızının biriktirme hızına etkisi reaktantların konsantrasyonu sabit tutularak araştırılmıştır. Buna göre, toplam gaz akışı biriktirme hızı ile ters orantılı olarak değişmektedir. Bu durum gazların reaktörde kalma süreleri ile açıklanabilir. Sonuç olarak, maksimum biriktirme hızı icin sıcaklık ve konsantrasyon oranı toplam gaz akışının 150 ml/dk oldugu durumda sırasıyla 1200 ^{o}C ve 0.050 ($[B_2H_6]/[NH_3]$) olarak bulunmuştur.

Anahtar Kelimeler: CVD, Bor Nitrür, BN, Tungsten

To My Family

ACKNOWLEDGEMENTS

Firstly, I would like to express my sincere thanks to my supervisor Prof. Dr. H. Önder Özbelge for his invaluable guidance and interest in this study.

I would like to express my gratitude to my co-supervisor Assoc. Prof. Dr. N. Aslı Sezgi for her invaluable help and encouragement during this study. She enlightened me at all the stages of this study and I appreciate her patience and support.

I would like to thank Duygu Gerçeker for her understanding and valuable friendships. I am also thankful to my roommates Eda Açık, Merve Çınar and Miray Gülbiter for their valuable friendship and encouragement.

I would like to thank Kaan Reyhan, Sevgi Ünel, Gözde Dönmez, Gökçe Eroğlu, Serkan Şahin and Burcu Gökbudak for their support and patience to my timelessness.

I would like to thank the technicians in our atelier for their technical support and brilliant solutions anytime I needed.

I would like to thank METU Central Laboratory for the analyzes that are used in this study.

I appreciate my friends across the Atlantic for their support and care. I owe them a lot.

I would like to thank my co-workers and managers in BOTAŞ for their understanding each time I asked to take off from work.

Lastly, I am grateful to my family for their infinite support especially when I could not see the light at the end of the tunnel. Without their love and constant support, it would be really hard to overcome the difficulties.

TABLE OF CONTENTS

LIST OF TABLES

TABLES

LIST OF FIGURES

FIGURES

LIST OF ABBREVIATIONS

CVD	Chemical Vapor Deposition
h-BN	Hexagonal Boron Nitride
PVD	Physical Vapor Deposition
PECVD	Plasma Enhanced CVD
LPCVD	Low Pressure CVD
DC	Direct Current
LCVD	Laser Chemical Vapor Deposition
MOCVD	Metal Organic Vapor Deposition
XRD	X-ray Diffraction
XPS	X-ray Photoelectron Spectrometer
SEM	Scanning Electron Microscope
RF	Radio Frequency
FTIR	Fourier Transform Infrared Spectroscopy
ATR	Attenuated Total Reflectance
SAM	Scanning Auger Microscopy
TGA	Thermogravimetric Analysis
FESEM	Field Emmission Scanning Electron

	Microscopy
TPD-MS	Temperatured Programmed Mass Spectroscopy
DSC	Differential Scanning Calorimetry

List of Symbols

R_F	Deposition Rate of the Film (g/min)
w_f	Final Weight of the Film (g)
w_i	Initial Weight of the Film (g)
Δt	Reaction Time (min)
P	Density (kg/m^3)
Q	Volumetric Flow Rate (m^3/min)
$\dot{M}$	Mass Flow Rate (g/min)

CHAPTER 1

INTRODUCTION

Boron nitride is a ceramic material which has promising application areas in different industries. Formerly, ceramic materials were selected according to their single dominant performance characteristic such as mechanical strength, thermal conductivity or optical property. However, today, multi-functional ceramic materials are preferred because of their wide range application areas such as; micro-electronics, polymer industry and aerospace applications. Boron nitride is one of these ceramic materials with its valuable physical and chemical properties. High mechanical strength, corrosion resistance, chemical inertness, oxidation resistance, thermal shock stability, large band gap and thermal conductivity are among these valuable properties [1].

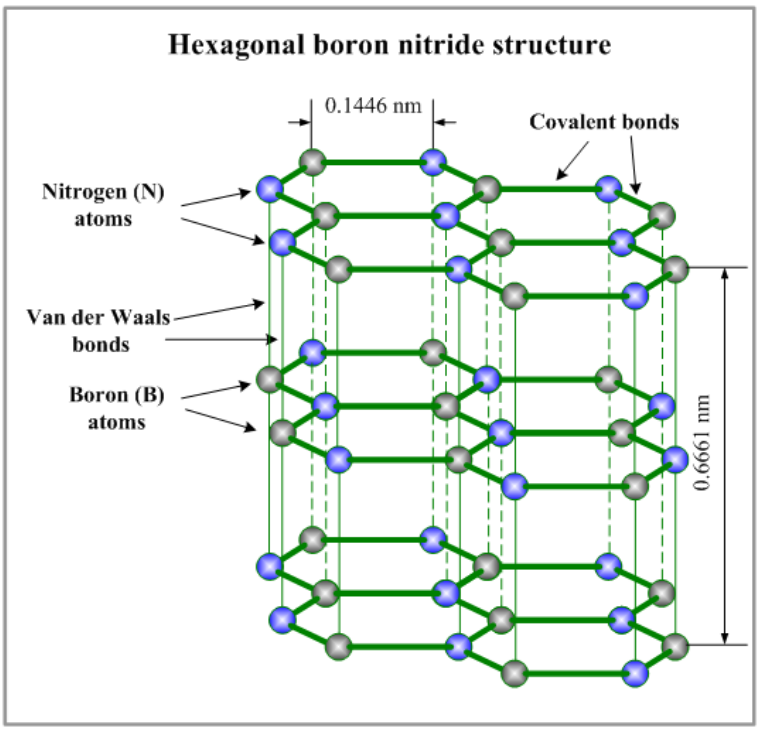

Figure 1.1. Layered Structure of h-BN [2]

As seen on Figure 1.1, the layered structure of h-BN shows very strong in-plane covalent but weak interplane (Van der Waals) bonding. This structure leads to anisotropic properties. More explicitly, properties of the material are different in ab and c directions within the material [1]. These properties are listed in Table 1.1 Moreover, layered structure of h-BN with weak interplane bonding provides lubricity, which makes h-BN popular at coating applications.

Table 1.1: Properties of Hexagonal Boron Nitride [1]

Molecular Weight (g/mol)	24.816
Color	White to Transparent
Density (g/cm^3)	2.1
Porosity (helium admittance) cm.sec	2×10^{11}
Thermal Conductivity(W/m.^oC)	ab 62.8 ; c 1.66 (at 100^oC)
Electrical Resistivity (Ω.cm)	ab 10^7 , c 10^{15} (at 1000^oC)
Dielectric Constant	ab 5.12; c 3.4
Hardness	Soft and lubricious
Compressive Strength (MPa)	c 234
Tensile Strength (MPa)	ab 41; c 103 (at 2200^oC)
Young's Modulus (GPa)	ab 22
ab: tested in ab direction (parallel to the surface)	c: tested in c direction (perpendicular to the surface)

As it can be seen on Table 1.1, h-BN can be produced as transparent and it creates different application areas such as production of x-ray masks, radar and infrared windows. It can be also used as interfacial layers for optoelectronic devices. Moreover, dopability of n- and p- junctions enables the material to be used for electronic applications on high temperature active device.

In polymer industry, h-BN can be added to the polymers as ceramic matrix component which helps to transfer external load, deflect matrix cracks, release residual thermal stresses and also prevent early failure of the fibers [3]. In addition to this, good resistance towards the repetitive thermal shock and self-lubricant property make it a strong candidate in aerospace applications.

h-BN also shows chemical inertness towards gas adsorption and other chemical processes; therefore, it can be used in coating of vacuum components' surfaces and reactor vessels. Besides these various application areas, h-BN can be also used in cosmetic industry [4,5,6].

1.1 Boron Nitride

Boron and nitrogen are neighbors of carbon element in the periodic table. Combination of these two elements has the same number of outer shell electrons with carbon element. For this reason, crystal structure of boron nitride is very similar to the crystal structure of carbon, in other words, boron nitride is isoelectronic with carbon element. Boron nitride has three crystal structures; hexagonal, cubic and wurtzite, as seen in Figure1.2. Carbon has two different crystalline structures; graphite and diamond which are analogous with hexagonal boron nitride and cubic boron nitride respectively.

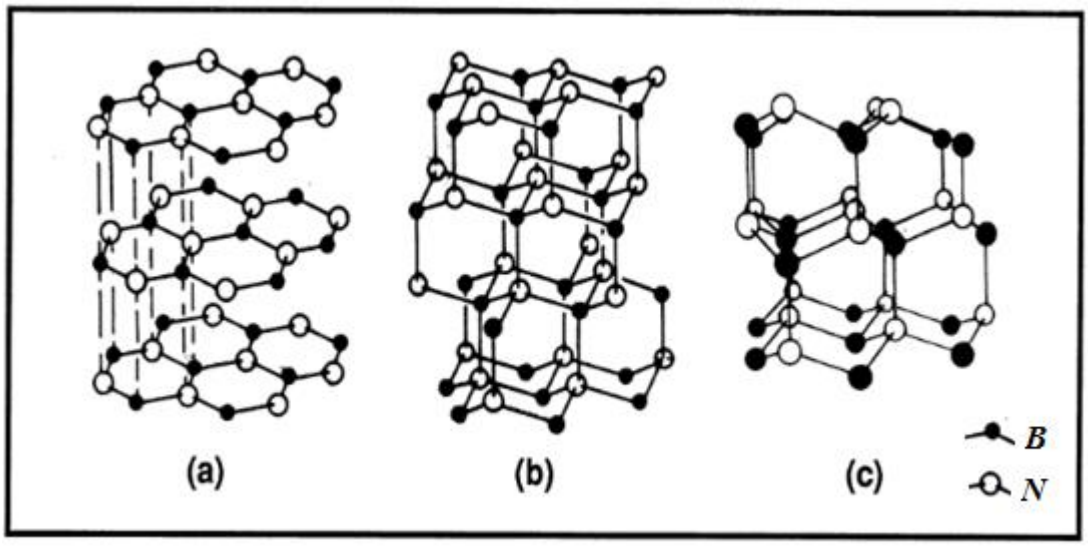

Figure 1.2. Boron nitride crystalline structures, (a) hexagonal, (b) cubic and (c) wurtzite [4].

Some of the crucial properties of the materials are based on their crystalline structure. For this reason, both diamond and cubic boron nitride are known as the hardest materials in the world. However, some of their other properties are quite different. For example, boron nitride is used as insulator in electrical applications; on the other hand, graphite has a good electrical conductivity. Graphite can be oxidized at low temperatures but h-BN has oxidation resistance up to 1300^{o}C. Moreover, unlike graphite, h-BN is a corrosion resistant material and has a very good chemical inertness [5].

1.2 Production Techniques

Chemical and physical properties of boron nitride highly depend on the purity of the precursors and production mechanisms. h-BN can be produced by using different methods such as Physical Vapor Deposition (PVD), Chemical Vapor Deposition (CVD) and Pyrolysis of Organics and other methods.

Chemical vapor deposition (CVD) is a process which involves gas-phase and surface reactions to produce solid phase products. In the chemical vapor deposition, the reactions can be activated by different resources. For example, activation energies of reactions can be passed over by using heat (Conventional CVD), UV (photo assisted

CVD) or plasma (PECVD or laser induced CVD) [7]. Precursors used in the CVD method should be in gas phases. However, in PVD, the reactants are in solid phase and the target material is evaporated and sputtered on the substrate under high vacuum in order to decrease the boiling point and it is more expensive method than CVD. In the PECVD method, precursors are activated by using plasma energy (20000 K) and the advantage of this method is to protect temperature sensitive substrates from high temperatures.

In the CVD processes, the reactant gases are converted to solid state products under the effects of chemical kinetics and fluid dynamic transport phenomena. There are two main CVD systems: closed CVD system and open flow CVD system. In the closed CVD system, there is pre-defined amount of reactants in a closed system which is surrounded by hot walls at which the chemical reactions occur and the product is adsorbed on the walls. In the open flow CVD system, reactants are fed to the system continuously and there is a surface at which the reactions take place. The thickness of the film can be determined by changing the continuous flow and the gas phase reaction products can be removed from the system. The most common system in the CVD processes is the open flow CVD system.

The nature of the deposition varies in different CVD processes. The slowest rate of the reactions can be controlled by mass transfer (diffusion) of the reactants to the surface (boundary layer phenomena) or by kinetics of the surface reactions. If the precursors can reach the surface rapidly (i.e. at low pressure) with enough amount, then the deposition rate depends on the surface temperature and kinetics of the reactions. On the other hand, if there is high pressure and high temperature in the system, the deposition rate is limited by mass transfer (diffusion) through the gas adjacent to the surface [8].

In our system, impinging jet reactor is used to minimize the effect of the mass transfer limitation; therefore, the kinetics of the reactions can be analyzed.

The chemical vapor deposition (CVD) method has many advantages in depositing thin films. Among these are dimensional variations, high purity of deposited material, well adherence of the film on the surface, higher deposition rate compared to PVD, temperature and pressure variations, composition and precursor variations.

All these make CVD the most preferred method in microelectronic and metallurgical manufacturing industry.

1.3 Chemical Vapor Deposition Reactor Types

Chemical vapor deposition reaction can be conducted in wide range of production systems for various application areas. There are mainly five types of CVD reactors; hot wall, cold wall, plasma assisted, laser or photon assisted and hot filament. All types of CVD reactors have similar mechanisms which include:

1. Gas delivery system in order to supply precursors to the reactor,

2. Reactor chamber where the reactions take place,

3. Substrate loading mechanism to place and remove the substrates,

4. Energy source to activate surface and gas phase reactions or decompose the precursors for the reactions within the reactor chamber,

5. Vacuum system to remove the undesired gas species from the system,

6. Exhaust system to remove the volatile by-products of reactions from the reactor chamber,

7. Exhaust treatment system (in case of harmful exhaust gases)

8. Process control equipment such as mass flow controller, temperature and pressure controllers to conduct the reactions and depositions within the determined deposition parameters.

1.3.1 Hot Wall Chemical Vapor Deposition:

In this type of reactor, heaters are placed on the outer wall of the reactor so that every part of the reactor is heated to the same reaction temperature as seen in Figure 1.3. For this reason, hot wall reactors provide the opportunity of multiple production and uniform thickness of the thin films. However, undesired coating on the inner wall of the reactor may cause depletion of reactive gases and higher thermal loads.

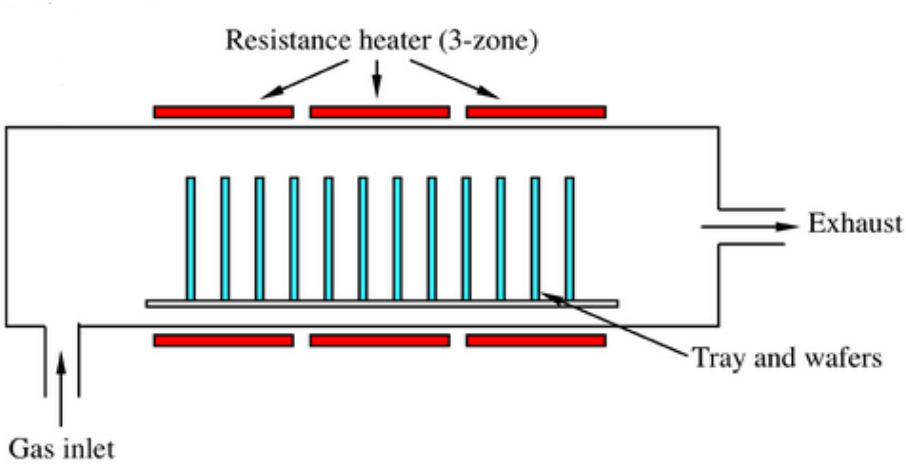

Figure 1.3. Hot Wall Reactor provides multi-wafer production [9].

1.3.2 Cold Wall Chemical Vapor Deposition:

Cold wall reactor is one of the most preferred reactor types in the CVD method. In this type of reactors, only the substrates are heated to the reaction temperature as seen in Figure 1.4. Many semiconductors which are used in microelectronics are produced by using cold wall reactor because cold wall reactor provides fast production (fast heat-up and cool-down processes) and energy efficiency due to low thermal load. Main disadvantage of this reactor might be the non-uniform temperature distribution on the substrate and possible thermal stress during heating-up and cooling-down processes.

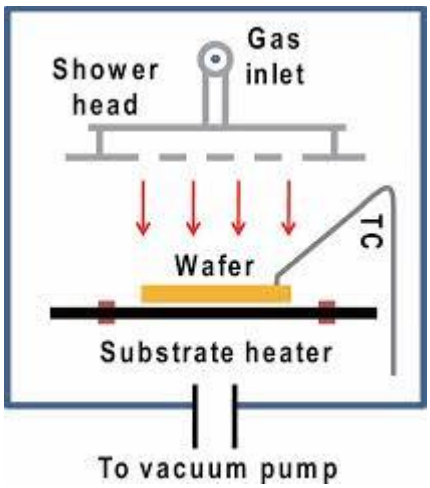

Figure 1.4. Cold Wall CVD Reactor with vacuum pump [10]

1.3.3 Plasma-Assisted Chemical Vapor Deposition:

Plasma-assisted CVD reactors are, in general, cold wall reactors. Reactions are activated using plasma, as seen in Figure 1.5, so substrate temperature does not need to be increased over 700K. In this type of reactor, plasma provides chemically active species such as ions and radicals from electron-molecule collision. This impacts the ions on the surface and thus, reactions take place. Gas temperature in the reactor remains between 25^{o}C and 350^{o}C so this reactor can be used in deposition processes on the polymeric substrates which cannot resist to high temperature. However, due to ion bombardment, surface damage can be seen on the film which leads to poorer film quality [11].

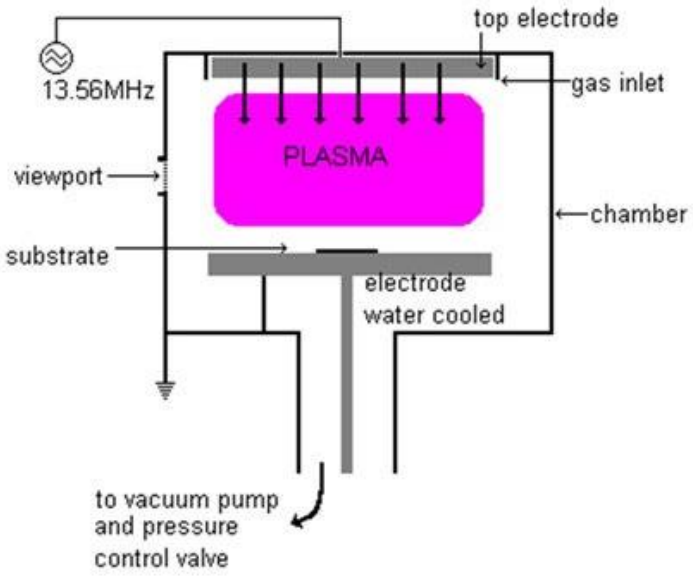

Figure 1.5. Plasma-enhanced CVD reactors are preferred for low-temperature substrates [12].

1.3.4 Laser Chemical Vapor Deposition

In this system, the shape and morphology of the deposited film are determined by laser process parameters. The difference between conventional CVD and laser-assisted CVD is laser matter interactions in the former one. There are two techniques in laser assisted CVD; photolytic and pyrolytic LCVD. In the photolytic LCVD the

precursors (reactants) absorb the laser to dissociate; on the other hand, in pyrolytic LCVD substrate absorbs the laser energy and creates hot spot which provides enough activation energy for the surface reactions of the reactants as seen in Figure 1.6 [13].

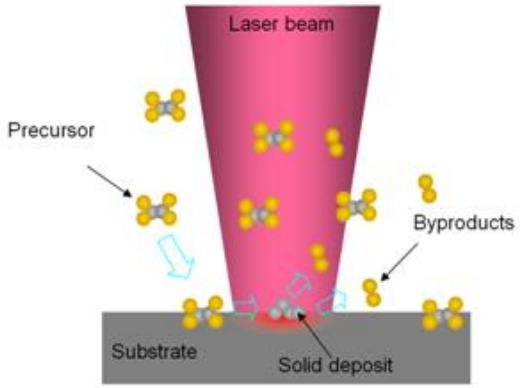

Figure 1.6. Laser assisted Chemical Vapor Deposition [14]

1.3.5 Hot Filament Chemical Vapor Deposition:

In this system, the energy source is the heat of the hot filament which has a high electrical resistivity. The temperature of the wire is increased by electrical connection, as seen in Figure 1.7, and the temperature might be more than 2200^{o}C. Each deposition method has its own advantages. For example, coating diamond on cutting tools for tribological applications are preferred to be produced by using hot filament CVD [15].

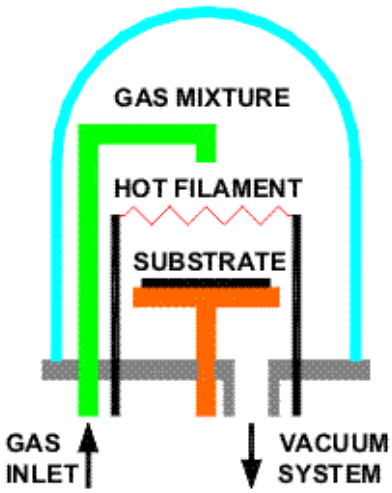

Figure 1.7. Hot Filament Chemical Vapor Deposition [16]

1.3.6 Metal Organic Vapor Deposition (MOCVD)

Metal-organic chemical vapor deposition has been used to produce Group III-V compound semiconductor materials and this process is also known as epitaxial growth. In this process, metal-organic precursors are fed to the system for the deposition reactions. Both Group III and Group V precursors are metal organic precursors. H_2 or N_2 can be used as a carrier gas to transport the precursors to the open tube process chamber as seen in Figure1.8. The purity of the precursors and the carrier gases are crucial for the quality of the deposited films [6].

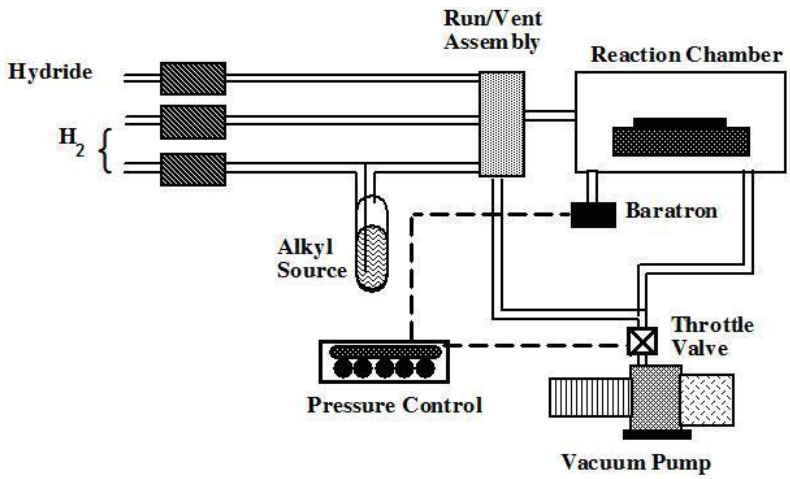

Figure 1.8. MOCVD Reactor Systems [17]

1.4 Precursors of CVD

Selection of the precursors is very crucial for pure and stable deposite. CVD processes are mainly based on decomposition and reaction of the gases on the substrate. Therefore, volatility of the precursors is very important to decompose at moderate temperature. For this reason, diborane is one of the best volatile precursors for CVD. It can decompose at room temperature. In addition, purity of the precursors has an important effect on the purity of the film and on possible gas phase reactions.

Various chemical combinations (precursors) can be used to produce h-BN via chemical vapor deposition method. The most popular ones are boron trichlorides (BCl_3) and diborane (B_2H_6) as boron sources, and ammonia as nitrogen source. Borazene ($H_3B_3N_3H_3$), TEB (Triethylboron)/NH_3, $Cl_3B_3N_3H_3$ (Trichloroborazene), $B_{10}H_{14}/NH_3$, BX_3/NH_3 are some other gas precursors to produce BN by using CVD method [1]. In these gas mixtures, nitrogen atoms in BN come from both ammonia and boron sources. BF_3/NH_3 gas mixture is not preferable because of byproduct, HF, which is strongly corrosive and damageable for the substrates. Although, deposition temperature of BN from BCl_3/NH_3 gas mixtures is approximately 500^oC, the product is unstable at the atmosphere of O_2 and H_2O. Moreover, for BCl_3/NH_3 gas mixtures, poor crystallization degree is obtained in deposited BN [6].

Diborane and ammonia are one of the best gas precursors for BN production in CVD. Lack of halogen atoms and oxygenated groups improve the purity of the deposit. The only impurity might be hydrogen atoms which are easily substracted by using heat annealing so that hydrogen content can be decreased [18].

1.5 Performance of CVD Systems

The performance of any CVD process can be evaluated using main aspects of the products.

1. Quality of the film: composition, interfaces, crystal structure and orientation of the film can be analyzed by XRD, Raman Spectroscopy, XPS and FTIR analysis. In addition, adhesion and film service life are also important for the film quality. Thermal and residual stress in film can be tested to determine the quality of the film after deposition.

2. Uniformity of the deposition: run to run uniformity for process reliability and repeatability, step coverage on features and shapes, microstructure and grain size uniformity are some of the considerations to determine the uniformity of the deposition.

3. Throughput of the CVD system: production rate and cycle time of the process, purge time for each process, heat-up, reaction and cool-down time, precursor conversion efficiency, equipment cleaning and maintenance, safety and other risks

during the process are some of the important factors to understand the smoothness of the process [6].

1.6 Mechanistic Steps of Chemical Vapor Deposition

The fundamental steps of a CVD process are shown in Figure 1.9:

1. Transportation of gas precursors in bulk flow into the reactor
2. Diffusion of reactant gases through the gaseous boundary layer to the substrate
3. Adsorption of gases onto the substrate surface
4. Single or multi-stage reactions on the substrate surface
5. Desorption of the product gases from the surface
6. Convective transport of gases from the surface

Modeling such a CVD process is based on the scientific foundations of fluid mechanics, thermodynamics, gas-phase kinetics and surface science. Especially at high temperature, gas-phase kinetics plays an important role to understand the whole CVD mechanism. There are various steps of the CVD process which make it difficult to determine the kinetics of the deposition reactions. Moreover, CVD processes are highly dependent on temperature, concentration gradient, geometric effects and gas flow pattern in the reactor chamber. As already mentioned, there are two main rate-limiting factors; mass transport and surface kinetics control.

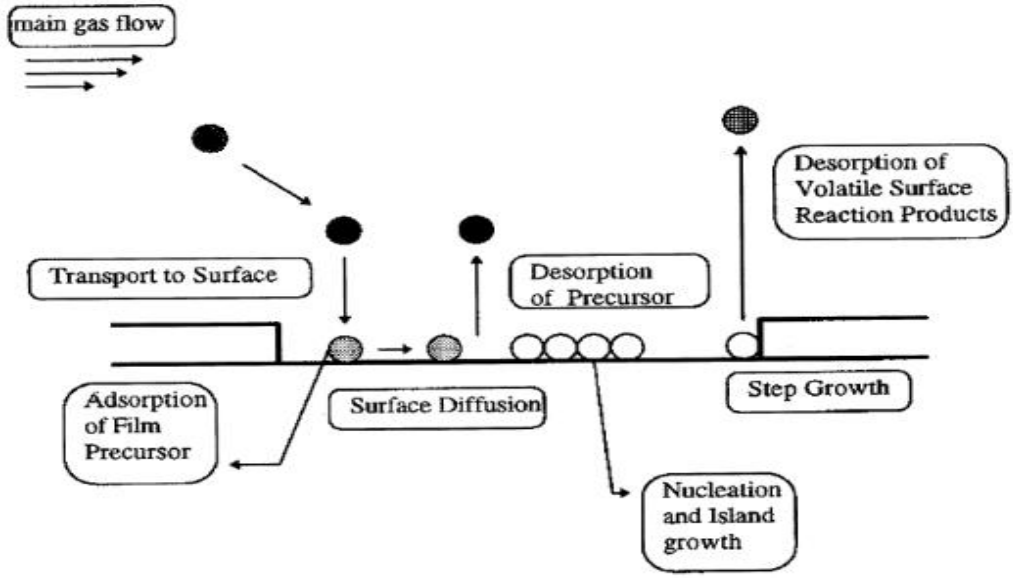

Figure 1.9. Mechanistic Steps of CVD [6].

Mass transport is dominant in thicker boundary layer on the surface to allow limited reactants or reaction products transferred from ambient to surface or vice versa. On the other hand, if boundary layer is not significant to control mass transfer, then surface reaction kinetics determines the rate [15].

In this study, impinging jet reactor is used to minimize the effects of mass transfer resistance (boundary layer) on the deposition kinetics. Deposition rate on the surface is expected to be independent from the mass transfer of the reactants through the boundary layer.

1.7 Literature Survey

Due to its unique properties such as chemical inertness, high electrical resistivity and high thermal conductivity, boron nitride has been investigated in many studies. In general, deposition rate, total flow rate and temperature parameters have been studied to show their effects on composition and crystalline structure of the product. Besides the studies on conventional CVD method, PECVD, DC arc jet CVD, RF coupled plasma CVD, LPCVD methods are also investigated in the literature. Chemical vapor deposition is one of the best methods to produce pure boron nitride for desired application areas because of easy optimization of parameters.

Aleixandre et al. [18] studied reaction of diborane and ammonia gas mixtures in a chemical vapor deposition hot-wall reactor on silicon substrate. In this study, deposition mechanism of boron nitride in a hot wall reactor by CVD and effects of temperature (600-800^{o}C) and gas flow ratio on the formation were shown. Reaction mechanisms are changing with different temperatures. At higher temperatures borazine is formed as an intermediate product and at lower temperatures aminodiborane is the intermediate compound. However, kinetic data and rate expression for proposed mechanisms could not be found.

Li et al. [19] prepared boron nitride coatings from borazine by hot-wall chemical vapor deposition (CVD) between 800 and 900^{o}C with a total pressure of 1 kPa. N_2 was used as carrier gas. The coatings deposited uniformly on the substrate at 900^{o}C and they were partially ordered h-BN. At 800^{o}C the coatings still contained some N-H bonds. On the other hand, 900^{o}C is high enough for decomposition of borazine completely. Crystallization of turbostratic boron nitride increased when the temperature increases above 1400^{o}C.

Aleixandre et.al. [20] studied influence of diborane flow rate on the crystalline structure and stability of boron nitride films by using chemical vapor deposition method. In this study, the experiment conducted at 800^{o}C and 267 Pa. The gas precursors were ammonia (NH_3) and diborane (B_2H_6) which is diluted in hydrogen (5% vol). Film was deposited on polished (100) silicon substrate. It is found that diborane flow rate affects the deposition rate. At low deposition rate, unstable film was observed in a moist atmosphere. At high deposition rate (high diborane flow rate), homogenous film composition and higher stability were observed.

Jin et al. [21] investigated the effects of temperature, pressure and feed rates of triethylboron and ammonia gases on deposition rate and characterization of BN thin films on crystal silicon substrate by using CVD method. Temperature range was 850-1100^{o}C and pressure range was 1 torr to atmospheric pressure. Argon and hydrogen gases were used as carrier gases. Partial pressure of TEB affects the deposition rate

with the power of 0.7 at atmospheric pressure. When the total pressure decrease while partial pressureof TEB and ammonia kept constant, the deposition rate increases due to increase in gas diffusivity. Up to 1050^{o}C, deposition rate increases with temperature then decreases with increasing temperature. XPS spectra showed that deposited films include carbon in carbide form and XRD analysis showed that films were of turbostratic structure.

Usamia et. al. [22] deposited boron nitride films on various metal substrates (Mo,W,Ni,Ti,Zr) by using DC arc jet CVD method with Ar-N_2-BF_3-H_2 gas mixture. Pressure was 50 Torr and temperature interval of the substrates was 850-1150^{o}C. As a result, it was observed that adhesion of BN films on Mo and W substrates was poor, and clear c-BN film Raman peaks were obtained. Different than Mo substrate, only a small amount of borides obtained at high temperature on W substrate due to low reactivity of W. When the production method compared with other CVD methods, ion bombardment caused higher stress in the films.

Andujar et al.[23] used capacitively coupled rf discharge (PECVD) method to deposite BN on different substrates such as fused silica, Corning 7059 glass, crystalline silicon polished on one and both sides and NiCr-coated silicon both on cathode and anode of electrodes. Two different gas mixtures were used; B_2H_6(1% v. in H_2) -NH_3 and B_2H_6 (5% vol. in H_2) -N_2. As results, for B_2H_6(1% v. in H_2) -NH_3 precursor deposited film on anodic surface was adhered very well and not scratched. However, deposited film on cathodic surface was easily scratched and flaked in atmosphere. Moreover, film stability of cathodic films worse than anodic films and that is determined by using infrared and optical transmittance spectra. On the other hand, this situation is opposite for B_2H_6-N_2 gas precursor. Therefore, properties and stability mainly depend on gas mixtures and substrate position (anodic or cathodic). Ion bombardment damaged the growing films by creating defects.

D. Franz et al. [24] studied effects of different gas mixtures Ar-B_2H_6-N_2 and Ar-B_2H_6-NH_3 on the formation of aminoborane products and BN using RF capacitively-

coupled plasma as an energy source. The RF power was 75 W and pressure was 0.5 torr. Film was deposited on silicon wafer and composition of deposited film was determined using XPS. As a result, it is observed that presence of ammonia in the gas mixture causes rich gas phase reactions and creation of some aminoboranes, and BN. On the other hand, in the case of presence of N_2 in the gas mixture, there was no indication of B-N absorption band in the plasma phase.

Cheng et al.[7] studied effects of gas composition and temperature on the amount and crystallize degree of deposite respectively by using LPCVD. Deposition kinetic of LPCVD BN production was examined. BCl_3-NH_3-H_2-Ar gas mixtures were used as gas precursor. As a result, deposition efficiency reaches 99.8% when NH_3 was used in excess. At 1000 ^oC and 1000 Pa, turbostratic BN was deposited onto graphite wafer. After heat treatment above 1300 ^oC, turbostratic BN converts into hexagonal BN and crystallization degree improved.

Choi et al.[25] studied deposition of h-BN films on graphite plates using cold-wall type quartz reactor heated by infrared radiation lamps in the reduced pressure. BBr_3-NH_3-H_2 gas mixture was used as gas precursor, NH_3/BBr_3 ratio kept constant as 3.0 and pressure was determined as 2, 4 and 8 kPa. Deposited film composition determined using Infrared spectroscopy and XRD. Surface morphology was displayed using SEM. As a result, deposition rate increases at lower pressure with increasing temperature. At 4 and 8 kPa, increasing temperature causes reactions in gas-phase and depletion of reactants so decreasing deposition rate. Deposited films cannot resist to atmospheric environment and turned opaque after a few days.

Ye et al.[26] studied h-BN coating from borazine on both Si(100) and SiBNC fiber wafers using hot-wall reactor under atmospheric pressure. Characterization of the coatings was determined using SEM, XRD and FTIR. The effect of temperature, reactant concentration and gas velocity on deposition rate was investigated. As a result, highest deposition rate was at 1090^oC, 20 vol% ammonia concentration and gas velocity of 10.5 cm s^{-1} (plug flow assumption). In a range of 0.081 vol% to 0.270

vol % concentration of borazine has no effect on deposition rate. Experiments were conducted with/without NH_3. Without NH_3, no h-BN coatings could be deposited. Moreover, SiBNC fibers were also successfully covered.

Frueh et al.[27] studied pyrolytic decomposition of ammonia borane (H_3NBH_3) to boron nitride. The thermal treatments (annealing) were done up to 1500^oC and H_2 was the major gas product, gas composition was identified by using TPD-MS. Deposited film was examined using ATR-FTIR and boron nitride product were analyzed in terms of composition, structure and morphology by using SAM, XRD, FESEM, TGA-MS, DSC. Infrared vibrational spectra were used to explain pathways of decomposition.

Dalui S. and Pal A.K.[28] studied deposition of boron nitride on Si (100) substrate at various substrate temperatures (400-600 K) by using RF plasma CVD method. Borane-ammonia, argon and nitrogen gas mixtures are used as precursors. FTIR is used to determine h-BN and c-BN compositions in the films. It is found that when temperature was increased, the composition of c-BN also increased. In this study, it is claimed that using inductively coupled plasma CVD the c-BN films can be deposited as a significant amount even though the common observation was the CVD method results lesser cubic phase of BN in the film.

Gafri O., Grill A. and Itzhak D.[29] studied deposition of BN on die steel and graphite substrates by using RF plasma method at temperature range of 550-620^oC. To characterize the composition X-ray diffraction and scanning electron microscopy were used. As a result, the coating was mostly amorphous but small amount of h-BN was also observed. The effects of deposition time and reactor pressure on growth rate were analyzed. The highest growth rate was observed at 2 Torr both on die steel and graphite. Also growth rate increased both on die steel and graphite with the temperature increased to 620^oC.

Zheng Y. and Wang S.[30] studied BN coating on quartz fibers using dip-coating in boric acid and urea solution at 700^{o}C. XRD, FTIR, XPS spectra and HR-TEM were used to determine the composition which showed polycrystalline h-BN properties. Thickness control was done by changing dip circles. In addition, mechanism of the reactions also was analyzed after applying heat process by using TGA which measures the weight changes. Morphology of the coating was analyzed using SEM, smooth and uniform coating was observed. It was found that thickness of the coating increased with dipping circle and theoretical thickness model was established during the study.

Li J., Zhang C. and Li B.[31] studied chemical vapor deposition (CVD) of borazine on carbon fibers at 900- 1150^{o}C. Scanning electron microscopy (SEM), Auger electron spectroscopy (AES), X-ray diffraction (XRD), FTIR and Raman spectroscopy were used to analyze the composition and the structure of the BN coatings. According to experimental results, maximum growth rate was 2.5μm/h at 1000^{o}C and the coating surface was loose and rough. Carbon element penetration from fibers to coating was also observed. It was found that below 1000^{o}C, deposition was controlled by surface reaction and at 1000^{o}C transition of surface reaction control to mass-transport control in the growth mechanism was observed. The degree of crystallinity of the coating increased with temperature increased and h-BN was seen above 1100^{o}C in the study.

S. Yuan et al. [32] studied production fluffy like BN spheres for catalyst support from ammonia and trimethoxyborane ($B(OMe)_3$) on sphere BN substrate by using the CVD method. There were two steps in this study. The first step was to produce sphere BN substrates from trimethoxyborane ($B(OMe)_3$) and ammonia at 1000^{o}C then was treated by ammonia flow at 1500^{o}C to produce sphere BN. In the second step, sphere BN particles were used as substrate in the presence of the same precursors of trimethoxyborane ($B(OMe)_3$) and ammonia. The temperature range was 1100-1400^{o}C in the second step to produce fluffy like BN. Characterization was done by using X-ray diffractometer (XRD), SEM, TEM and IR spectrum. As a

result, fluffy like (coarse surface) BN particles were produced to use in catalyst supports applications.

M. Karaman et al. [33] studied chemical yield, morphology and hardness of β-rhombohedral boron carbide (B_4C) on tungsten substrate in a dual impinging-jet chemical vapor deposition reactor. In this study, on-line FTIR analysis was used to analyze the chemical yield of boron carbide, 13% chemical yield of boron carbide was found and it can be increased with an increase in temperature. XRD analysis showed that at 1300°C, pure rhombohedral B_4C phase can be obtained without any other phase or impurities. The crystalline structure of the product which is highly symmetric provides very high hardness value of 4750 kg/mm^2.

Sezgi et al. [34] studied CVD of boron by hydrogen reduction of BCl_3 on a hot tungsten substrate in a parallel flow reactor. Effect of substrate temperature (1100°C-1250°C) on the deposition rate of $BHCl_2$ and boron was investigated to show the crystalline structure with different temperatures. It was found that α-rhombohedral boron with large crystals and sharp facets can be obtained at 1100°C and β-rhombohedral boron with small crystal size can be obtained at 1300°C. The comparison between impinging jet reactor and parallel flow reactor shows that there was a significant mass-transfer resistance in the parallel flow system which decreases the conversion of BCl_3 to boron.

Sezgi et al. [35] studied the mechanism of boron deposition by hydrogen reduction of BCl_3 in a dual impinging-jet reactor. FTIR analysis was done on effluent gas mixture to collect information about kinetics of the gas phase and surface reaction kinetics. Formation of $BHCl_2$ was found as intermediate product. The experiments were conducted at the temperature range of 750°C-1350°C. The collected data indicated change of reaction mechanism at around 900°C. At higher temperatures, boron formation might be seen as the decomposition of BCl_3 without hydrogen reduction.

Dilek et al. [36] studied the formation of boron carbide on tungsten substrate from BCl_3, H_2 and CH_4 in a dual impinging jet reactor. The experimental data showed that $BHCl_2$ and β-rhombohedral B_4C were formed as intermediate product during the formation of boron carbide. Molar ratio of BCl_3/CH_4 determined the conversion of B_4C, increase in molar ratio increases the conversion rate. The reaction rate of B_4C formation was proportional to the 1.85 power of the BCl_3 concentration.

Özmen et al. [45] studied the synthesis of boron nitride nanotube (BNNTs) from ammonia and a powder mixture of boron and iron oxide in a tubular reactor. XRD analysis showed that h-BN and rhombohedral boron nitride, iron, boron oxide and iron boride were formed in the product at different temperatures and gas composition. Mass spectrometer (MS) was used for the chemical analysis of outlet gas. MS results showed that the only gas phase reaction was the decomposition of ammonia. SEM and TEM images proved the BNNTs formation in the product.

1.8 Objective of the Study

In previous studies, there is no information related to boron nitride production on tungsten substrate using chemical vapor deposition method. Boron nitride has been produced on different substrates, using different precursors with CVD methods. The kinetics of the reactions is controlled by both gas phase reactions and surface reactions in these studies and it affects morphology and deposition rate of the film.

Considering the originality of the study, the main objective is to produce boron nitride thin film on the tungsten substrate. In order to achieve this, CVD reactor is constructed, in which mass transfer resistance is minimized using impinging-jet reactor. The main objectives of this study are to:

- Produce of boron nitride on tungsten substrate
- Characterize of the produced film in terms of crystalline structure and morphology
- Investigate the effects of substrate temperature, composition and total flow rate of the precursors on the BN deposition rate

CHAPTER 2

EXPERIMENTAL

In this study, production of boron nitride on tungsten substrate consists of two main experimental parts:

1. Production of the boron nitride film on tungsten substrate

2. Characterization of the produced film to collect information about crystalline structure and morphology

In order to study the effects of temperature, molar ratio of reactants and total gas flow rate on the deposition rate and characterization of the film, in total 37 experiments were conducted (including repeatability experiments).

2.1 Experimental Set-up

Different types of CVD processes can be used to control deposition rate and film quality. In order to maximize deposition rate and minimize mass transport limitations, an impinging jet reactor is used (Figure 2.1) in this study. The reactor was designed by Sezgi et al. [37].

Experimental set-up is shown in Figure 2.2 schematically. It is established in an explosion chamber which has a good ventilation system because diborane and ammonia are highly dangerous and toxic. The system is very similar to the system which was designed and used by Sezgi et al. It consists of three main parts: gas inlet, reactor and gas outlet. There are two inlet tubes to feed the reactor; diborane (B_2H_6), ammonia (NH_3) and argon (Ar). Diborane gas mixture includes 10% diborane and 90% of H_2 (Linde) in order to prevent decomposition of diborane. Ammonia gas mixture (Linde) is highly pure (with 99.999%). Argon is used to purge the system at

the beginning and at the end of the each run and is also used during the experiment as an inert gas. Flow rate of the gases are controlled and arranged with mass flow controllers (Aalborg GFC 17) which are designed specifically for diborane, ammonia and argon gases.

In order to be precise, calibration of the mass flow controllers is performed via soap bubble meter (Appendix A). Precursor gases are fed to the reactor through stainless steel piping system and brass piping system. Piping system is designed according to gas types. For example, diborane and ammonia are highly corrosive gases; therefore, stainless steel piping system is used for those gases. On the other hand, for argon, brass piping system is preferred as a result of its being easily shaped.

There is a union cross fitting element to mix the three gases before entering the reactor as seen on Figure 2.2. Until the pipe cross, the piping system is made of ¼ inch stainless steel tube. After that mixing part, brass piping is used (diborane and ammonia are diluted in argon and they are not as corrosive as pure diborane). Moreover, there is an on/off valve before the reactor for safety reason. In any emergency case in the reactor, the inlet gas mixture can be stopped using this valve.

Inlet gases are fed to the dual impinging jet reactor from both sides of the reactor, as shown in Figure 2.1. The diameter of the reactor is 1 cm and there are orifices just before the gases reach to the surface in order to minimize the mass transport limitations and the diameter of the orifices is 1 mm. There are two stainless steel electrodes which have one hole each to hold tungsten foil. The diameter of the upper electrode is 1.60 mm and the diameter of the lower electrode is 2.03 mm. The upper electrode is connected to DC power supply using tee fitting element. The lower electrode sinks into the mercury pool to complete the circuit. The weight of the lower electrode provides smooth tungsten surface. Surface of the substrate is aligned in the middle of the reactor and the distance between the surface and the orifice is 0.5 cm.

The reactor is made of quartz to resist high temperatures (up to 1250^{o}C) and is placed in a plexi-glass cell for protection. There are two holes on this cell; one is to feed the inlet gases to the reactor and remove the effluent gases from the reactor and the second one is to connect DC power supply to the reactor as energy source. There is also another ventile system on the cell to remove any gas leakage from the system.

Effluent gas can be controlled and measured using soap bubble meter. After soap bubble meter all the product and reactant gases are vented out from the system to the atmosphere.

As it is mentioned before, DC power supply is used as energy source in this reactor. It provides energy using the principle of the resistivity of the metals which are held in the reactor. By arranging voltage and current rate, the temperature of the substrate can be controlled.

Tungsten is used as substrate in this study because it can resist to high temperatures (up to 3430^{o}C) and also it has high resistivity which helps to increase the temperature of the surface using DC power supply. The substrate thickness is 0.025 mm and it has 99.95% purity. It is placed between two stainless steel electrodes with the help of tungsten wire.

Optical pyrometer is used to measure the temperature of the substrate during the experiment. There is a temperature distribution along the surface so three data are taken from upper part, middle and lower part of the substrate surface. Value of arithmetic average of those three data is the surface temperature.

In this study, effects of temperature, residence time and B_2H_6/NH_3 molar ratio on film quality and deposition rate were studied. The most important property of impinging jet reactor is to decrease mass transfer boundary layer thickness around 30 fold compared with conventional CVD reactors. Indeed, in conventional CVD reactors deposition rate is limited by diffusion rate in other words mass-transport rate. However, in order to maximize deposition rate surface kinetics should predominate during deposition.

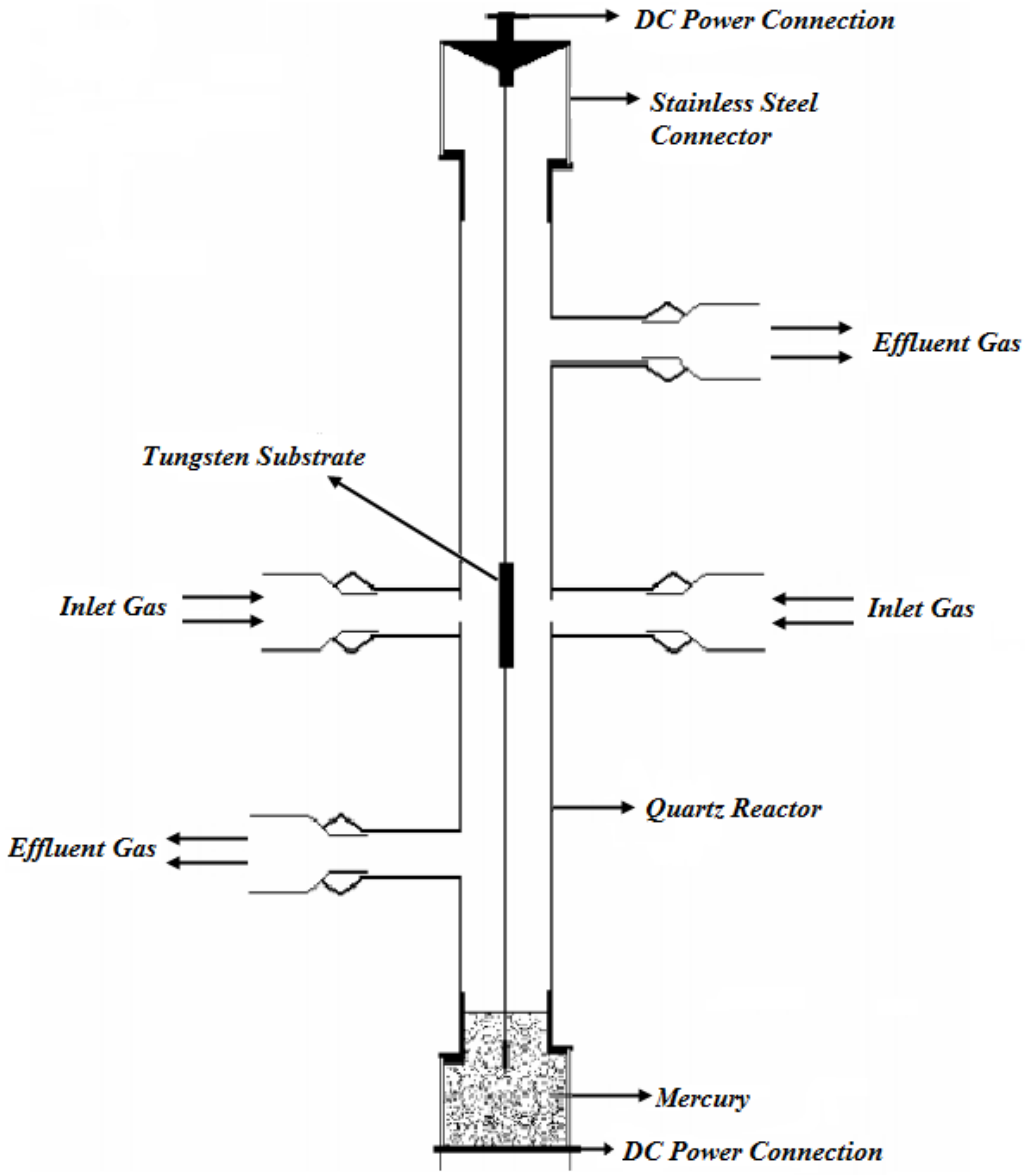

Figure 2.1. Dual Impinging Jet CVD Reactor [37]

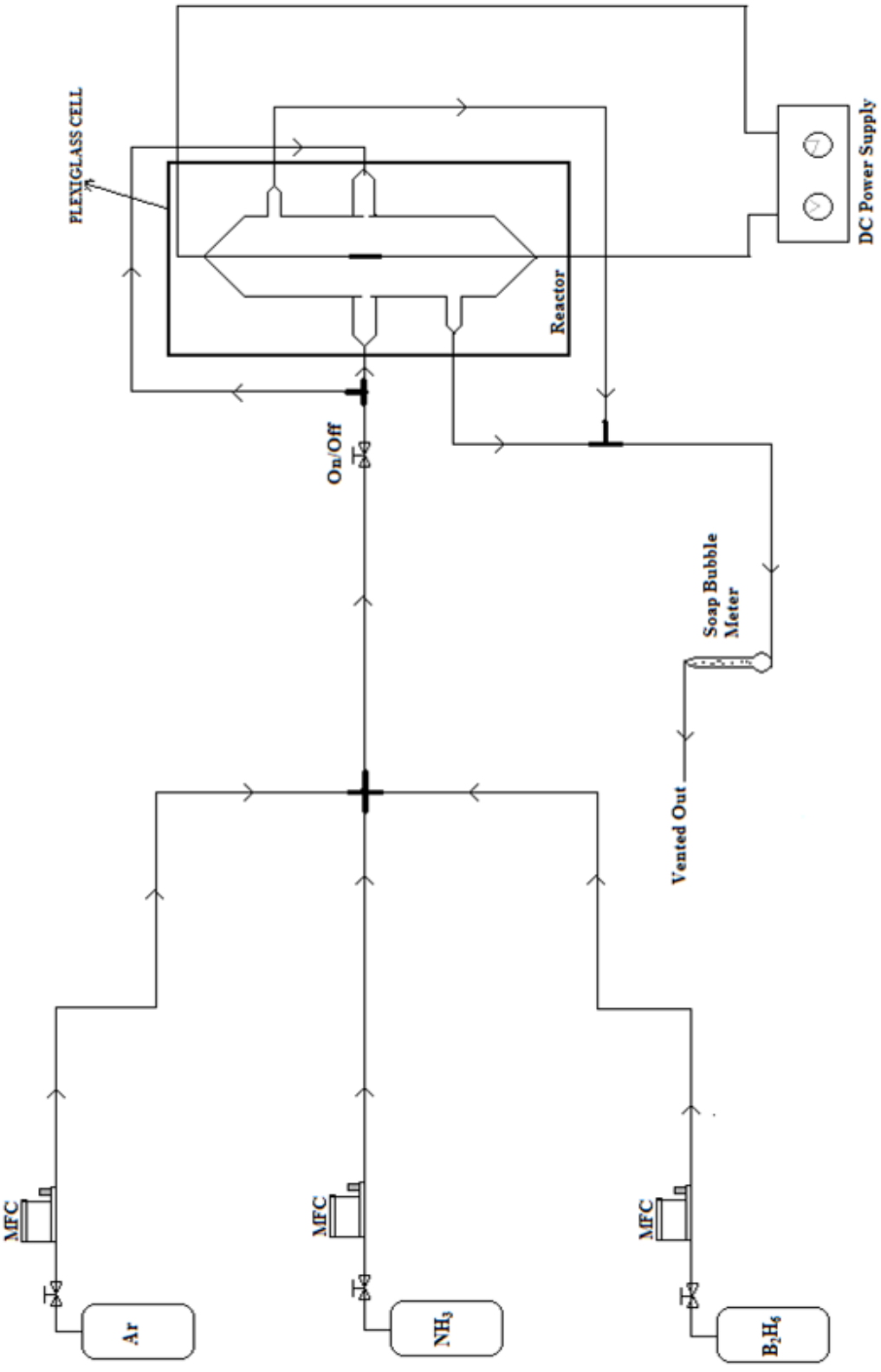

Figure 2.2. Experimental Set-Up

2.2 Experimental Procedure

Temperature, molar ratio and total gas flow rate parameters are studied in this study as seen on Table 2.1. At the beginning of the each run, tungsten surface is prepared from 100mmx100mm foil. The size of the surface is 2.5 cm (length) x 2.2 mm (width). It has 0.025 mm thickness. The length of the surface between two electrodes was 1.2 cm. Before placing the foil in the reactor, it is needed to weigh with precision scale. It is recorded as the initial weight of the film. Then tungsten foil is placed into the reactor with the help of tungsten wire. After it is held by the electrodes, multi meter is used to see whether the path of electric circuit is completed or not. If the circuit is completed then DC power supply is connected to the system.

First, argon gas is fed to the system at 2 bar to purge and remove all the impurities from the reactor. It may take 30 to 45 minutes. Then, ammonia gas is fed at 2 bar to the reactor and total flow rate is measured with soap bubble meter to check the values of the mass flow controllers. After ammonia gas reaches to the desired flow rate level, diborane is fed at 2 bar to the reactor and total gas flow rate is measured with soap bubble meter again.

Diborane and ammonia are fed to the system with argon because of their high corrosive effect. It may harm the piping system. Especially, diborane should not be fed alone because it might decompose and accumulate in the reactor chamber or in the piping system. After total flow rate becomes stable and constant (it may take even 1.5 hours) DC power supply can be turned on and the voltage and current rate can be arranged to reach the desired surface temperature.

After arranging the voltage and current rate, optical pyrometer is used to measure the temperature of the surface. Each run is 60 min long and every 5 minutes the temperature is measured.

During the experiment due to the deposition of the film, the measured temperature decreases so the voltage needs to be rearranged. In order to keep the surface temperature constant the time interval to measure the temperature of the surface is at every 5 min.

After completing 60 minutes for the run, the DC power supply is disconnected from the reactor so the temperature of the surface decreases immediately. Therefore, it can be assumed that there are no more surface reactions taking place on the substrate after the disconnection. Then, diborane and ammonia gas valves are closed using regulator and argon is fed to purge the gases from the reactor chamber.

After purging the system, the reactor is opened and the tungsten substrate is removed from the reactor. The weight of the foil is measured using precision scale and it is recorded as final weight of the film. The difference between final weight and the initial weight provides us the information of the deposition amount of boron nitride.

Experiments are conducted at different temperature, molar ratio of reactants and total gas flow rate, the parameters for those experiments can be seen in Table 2.1. The molar ratios of reactants are calculated in Appendix B.

Table 2.1: Experimental parameters to collect information about the structure and morphology of produced Boron Nitride films.

Temperature (^oC)	Molar Ratio (B_2H_6/NH_3)	Total Flow Rate (ml/min)	Number of Repeatability
900	0.050	150	3
1000			6
1100			5
1200			9
1100	**0.033**	150	7
	0.050		5
	0.099		4
1100	0.050	**100**	1
		125	1
		150	5
		175	1

2.3 Characterization Techniques

Boron nitride film on tungsten substrate can be produced using the chemical vapor deposition method in impinging jet reactor as explained in the experimental procedure (part 2.2) however, it is crucial to collect information about the morphology and composition of the film after each experiment. In this study, the main objective is to produce boron nitride thin film on tungsten substrate so XPS (X-ray Photoelectron Spectrometer) can provide atomic weight ratio of the elements within the film and the composition can be determined using this information. Raman spectroscopy is useful to confirm presence of BN in the film deposited. Crystalline structure of the film can be revealed using XRD method. SEM (Scanning electron microscopy) can be used to see the images of the film surface to assess the morphology of the film. Finally, thickness analyses can be done to compare the profiles of the deposited films

2.3.1 X-ray Diffraction (XRD)

X-Ray Diffraction method is used to measure intensities of the diffracted radiation. The main purposes of the measurement are;

i. Determination of periodicity, symmetry and orientation of a crystal.

ii. Accurate estimation of intensities to explain atomic arrangement within asymmetric unit in other words its structure.

XRD measurements are based on electromagnetic radiation with wavelengths range of 0.02 A and 100 A. Compared with the wavelengths of X-rays to visible light, it is much smaller so the energy and penetration power of the X-rays are higher and it can penetrate to the sample matter to characterize its structure [40]. In this study, CuKa1(λ:1.5406 A) tube and Ultima IV Riyaku In-plane goniometer is used with continuous scanning (2θ) between 10-100 and scan speed of 1.0 deg/min. The X-Ray energy has 40kV/30mA and 10 mm window is used during the scanning.

2.3.2 X-ray Photoelectron Spectrometer

X-ray Photoelectron Spectrometer is used to collect information about the composition, electronic state of solids, oxidation states of transition metals, identification of elements near the surface and surface composition, valence band electronic structure, morphology of the thin films. The principle of XPS is based on photoelectric effect. Each element on the surface of the sample has core electron with specific binding energy which is equal to ionization energy of that electron. If the energy of the photon is higher than the ionization energy then the electron is emitted from the surface and can be detected [38]. In this study, PH1 5000 VersaProbe ULVAC-PHI. INC with AlKα tube is used to analyze the composition and atomic weight of the elements in the composition. The sample was sputtered with Argon during 2 minutes to remove the impurities on the surface.

2.3.3 Raman Spectroscopy

Raman spectroscopy measures the energy of shifted photons depending upon the vibrational state of the molecules which provides chemical and structural information about the molecules in the sample. There is no need to sample preparation; energy is measured by scattering rather than transmission or reflection [46]. In this study, Renishaw/Invia Dispersive Raman device was used with the laser of 532 nm Nd. YAG and the power of the laser was 100 mW. The magnitude of the zoom for scanning was 50X (Figure 3.6)

2.3.4 Scanning Electron Microscope (SEM)

High energy electrons are used to create signals from the interaction with the sample surface. This signal gives information about the surface texture of the film in scanning electron microscope (SEM) technique. Areas which are analyzed can be ranged between 1cm to 5 micron in width [42]. In this study, the samples are covered with gold (Au) to provide conductivity during the scanning. The SEM images are taken with the

magnitude of zoom in 100000x and the focused area was selected as the middle of the each sample.

2.3.5 Thickness Analysis

Thickness analysis is done to collect information related to the film profile on the substrate. Digital caliper is used for the measurements. In this study, TIME (ABSolute Series 110-15DAB) digitonic caliper was used. Five points along the film surface were selected. The profiles of the films are shown in Figures 3.18 & 3.19 in the vertical position.

CHAPTER 3

RESULTS AND DISCUSSION

Boron nitride (BN) production on tungsten substrate is produced from ammonia (NH_3), diborane (B_2H_6) and argon (Ar) gas mixture in impinging jet-reactor at different substrate temperatures. Morphology of the film and the composition are examined using SEM and XRD, Raman Spectroscopy and XPS analysis. The effects of temperature on deposition rate and morphology of the film are investigated by conducting the experiments at different surface temperatures. In addition, the effect of total gas flow rate on deposition rate is also analyzed keeping the molar concentration of the reactant gases constant.

3.1 XRD Analyses Results

3.1.1 Effect of Temperature

XRD peaks of produced film can be seen in Figure 3.1. Four samples, produced at different temperatures, were analyzed to collect information about the structure of the film. XRD data of the analyzed films is given in Appendix C.

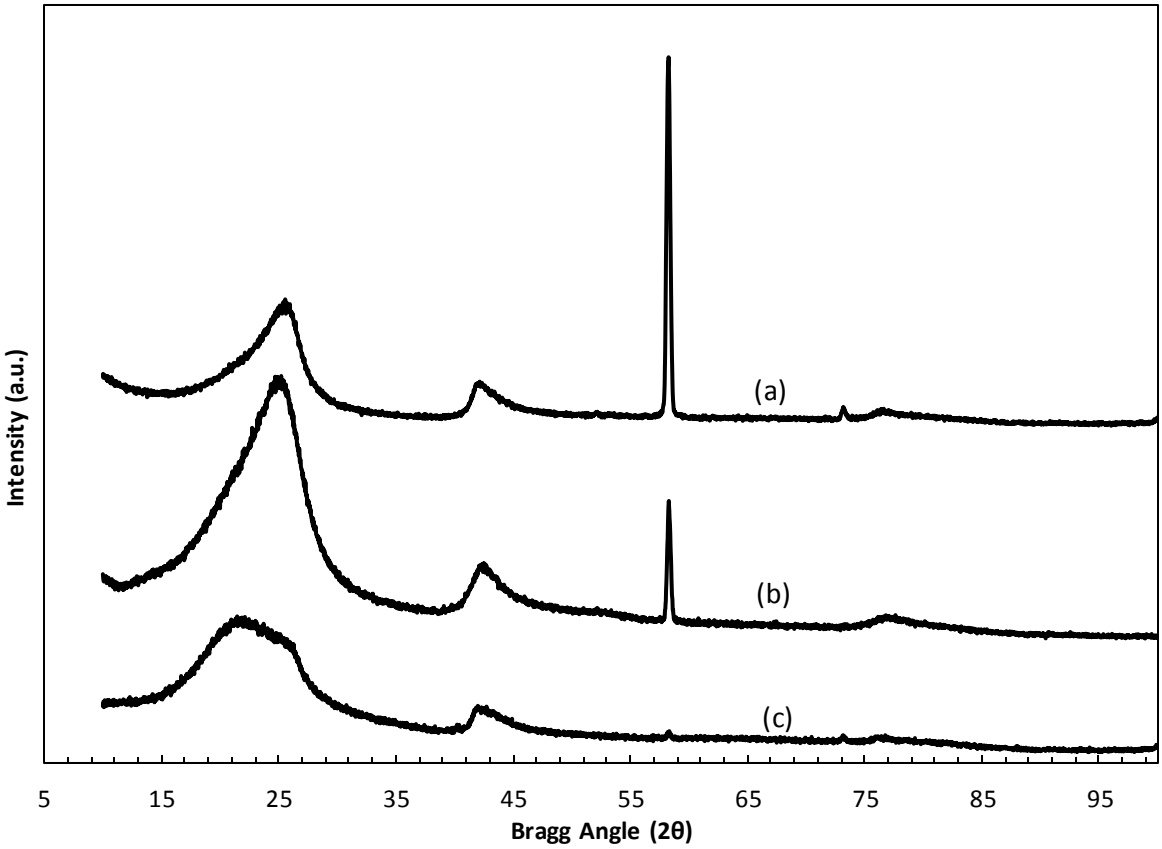

Figure 3.1. XRD patterns of the films produced with B_2H_6 to NH_3 molar ratio of 0.050 and total flow rate of 150 ml/min at different surface temperatures (a) 1000°C (b) 1100°C (c) 900°C

As seen in Figure 3.1, peaks around 25.5° and 42.5° and 76.4° show the diffraction of h-BN. The first peak comes from the diffraction of (002) plane and second peak comes from the diffraction of (100) and (001) planes. These results are consistent with the XRD analyzses of h-BN in the literature [19]. Peaks at 58°, 73° and 78° belong to tungsten (Appendix F). In some of the patterns, tungsten peaks cannot be seen due to the fact that X-ray may not be incident on the tungsten.

When the patterns are compared between two samples produced at 1000°C and at 1100°C in Figure 3.1, they showed differences in terms of intensity and width of peaks which can be explained by the amount of BN in the film, particle size and the effect of temperature on the crystallinity.

Pattern of the film produced at 900°C show a broad diffraction in the first peak and the maximum of the peak is at 22° (Figure 3.1.c) on the other hand other patterns have their maximum peaks are at 25.5°.

In fact all peak intensities of BN increase with temperature and width of peaks produced at 900°C, 1000°C and 1100°C are large, that means that the composition of the deposit contains boron compounds other than BN.

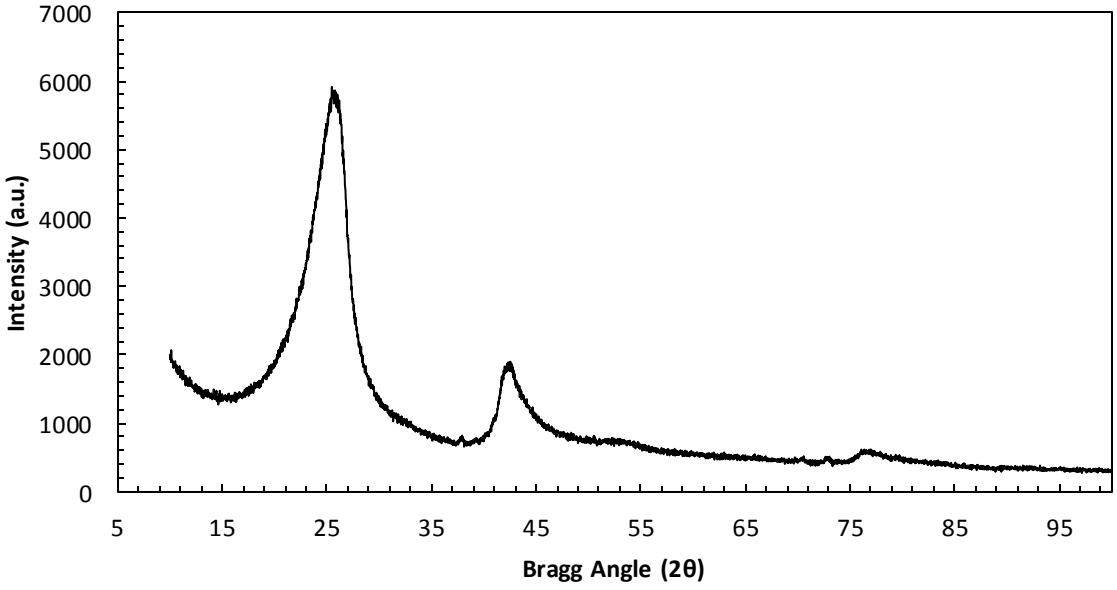

Figure 3.2. XRD pattern of boron nitride produced at 1200°C (powder)

The pattern of boron nitride produced at 1200°C gives the peaks at Bragg Angle (2θ) values of 25.5°, 42.5° and 76.4°.

Boron nitride produced at 1200°C was analyzed in the powder form to obtain XRD pattern in the absence of tungsten substrate. It is narrow compared with other three patterns for different temperatures the reason might be the high h-BN content and powder form of the analyzed sample. Intensity of first and second peaks of boron nitride produced at 1200°C is higher than other XRD results as well.

Comparison of the patterns gives some valuable information about how the temperature affects the crystal structure of the deposited film. XRD results show clearly that the h-BN film (on the tungsten substrate) and other solid boron components might be formed as well.

3.1.2 Effect of B_2H_6 to NH_3 Molar Ratio

The XRD patterns produced at 1100°C and with the total flow rate of 150 ml/min gave peaks at 25.5°, 42.5° and 76.4° for $[B_2H_6]/[NH_3]$ ratios of 0.033, 0.050 and 0.099 as seen in Figure 3.3. That shows the deposition of h-BN. The peaks at 58° and 73° belong to tungsten.

Width of the peaks shows low boron nitride crystallinity and other boron compounds in the material cause broad diffraction. It should be noted that h-BN peaks are similar with the peaks obtained at different temperature XRD patterns.

Comparison of the patterns gives some information about how different molar ratios $[B_2H_6]/[NH_3]$ of reactants affects the crystal structure of the deposited film. It can be claimed that at the molar ratio of 0.033 and 0.050 the places of the peaks show similarities. However; at the molar ratio of 0.099 due to NH_3 deficiency other boron components might be formed on the film which causes broad diffraction angles.

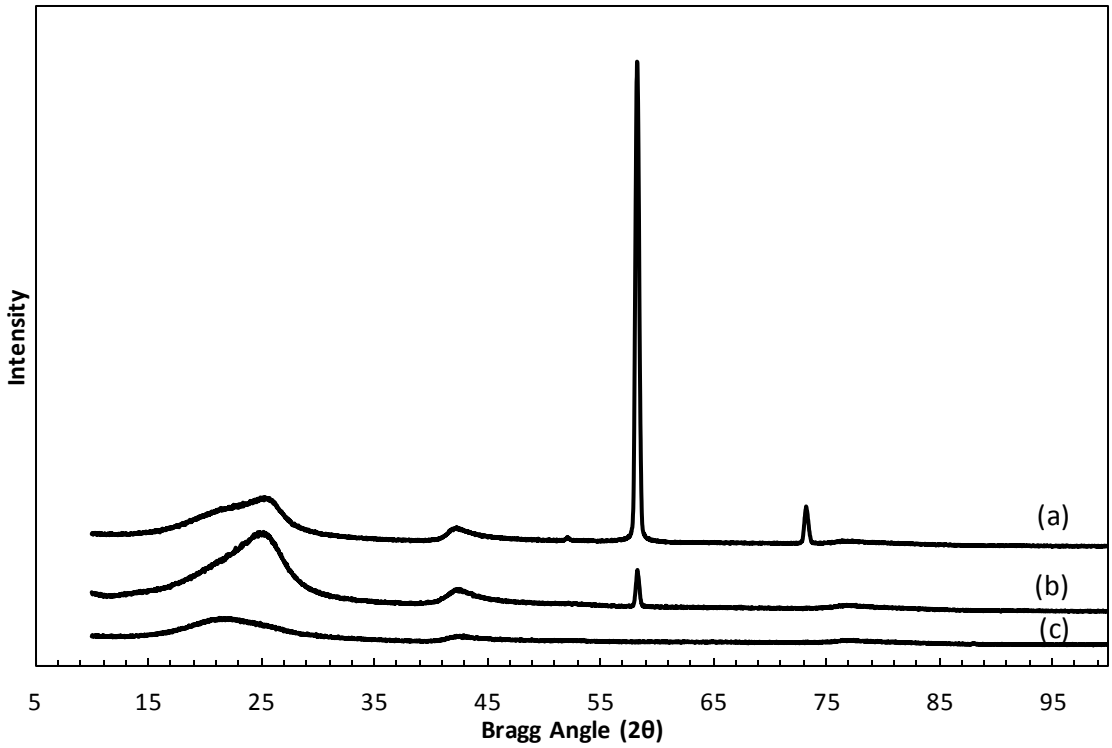

Figure 3.3. XRD patterns of deposited film produced with molar ratios $[B_2H_6]/[NH_3]$ of (a) 0.033 (b) 0.050 and (c) 0.099 at 1100^oC with the total flow rate of 150 ml/min.

According to Figure 3.3, intensity and width of the peak values of the material produced with the molar ratio of 0.050 is larger than the other two patterns of boron nitride, which shows that, crystallinity and deposition amount of boron nitride increase when the system is fed with the reactants at the molar ratio of 0.050.

3.1.3 Effect of Total Gas Flow Rates

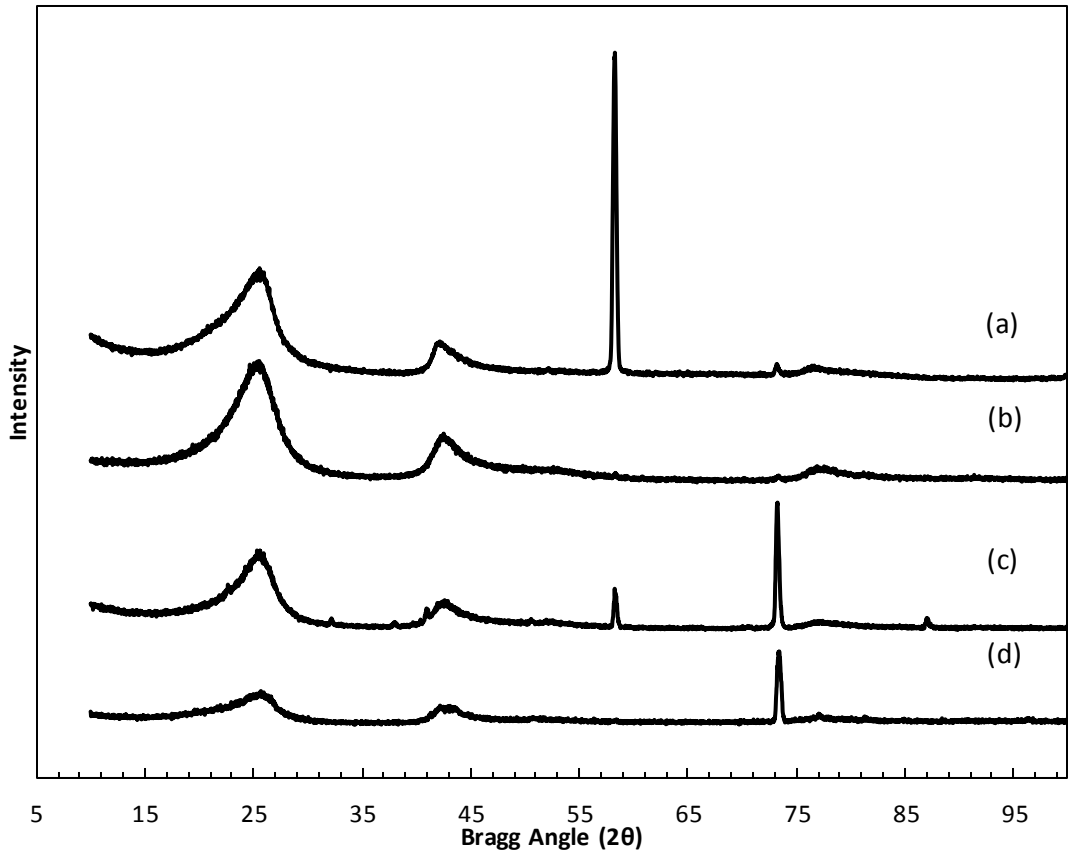

Figure 3.4. XRD patterns of boron nitride produced with total gas flow rates of (a) 150 ml/min (b) 125 ml/min and (c) 100 ml/min and (d) 175 ml/min at 1000°C with the molar ratio $[B_2H_6]/[NH_3]$ of 0.050.

As seen in Figure 3.4, the patterns of the films produced with different total gas flow rates have similar diffraction angles around 25.5°, 42.5° and 76.4°.

At 175 ml/min (the highest studied), the structure of the boron nitride shows less crystalline structure (Figure 3.4.d). Due to narrow width of peak value and high intensity of the pattern, the film produced with the total flow rate of 125 ml/min shows that the amount of deposited BN is higher compared with other samples (Figure 3.4.b). The compositions of the films are similar according to position of the peaks. Broad

diffraction may be interpreted as the formation of other boron compounds in the deposit and different particle size.

When the two figures (Figure 3.4 & 3.1) are compared, it can be seen that the change in total rate does not affect the sharpness of the XRD peaks as much as change in temperature. This means that total flow rate is not an effective parameter on the crystallinity of films.

3.2 Raman Spectroscopy Result

Raman Spectroscopy analysis was done to determine the bonds and it can be used to find fingerprints of the molecules.

As it can be seen in Figure 3.5, the Raman spectrum of boron nitride film produced at 1100^{o}C shows its highest peak at 1376.46 cm^{-1}. This spectrum can be compared with studies in the literature. One of the studies done using different boron and nitrogen sources on tungsten surface shows that h-BN has its highest peak around 1375 cm^{-1} [22].

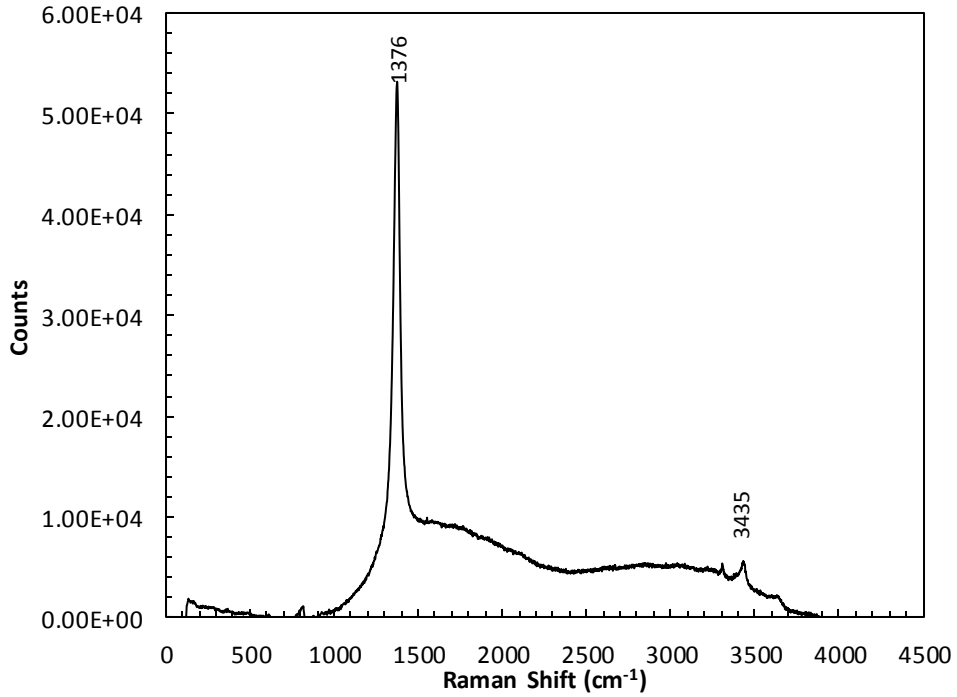

Figure 3.5. Raman Spectrum of deposited film produced at 1100^{o}C.

The other three peaks can be identified by looking at the literature. For example, water molecules have stretching vibrations at around 3435 cm^{-1} (O-H bonds)[44]. This peak may come from water molecules in the BN film which is a wettable product. The view of the BN film analyzed in Raman spectroscopy can be seen in Figure 3.6, which shows that the film has rough surface.

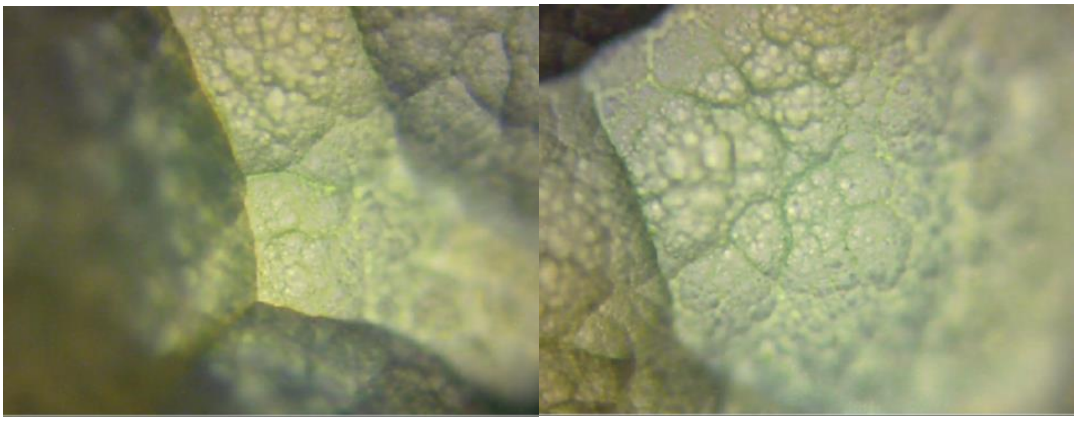

Figure 3.6. View of the produced film with Raman Microscope. The magnitude of the zoom in these images is the same at 50X.

3.3 X-ray Photoelectron Spectrometer Analysis Result

XPS analysis of the produced BN can be seen in Figure 3.7. It can be used to predict the possible compositions in the product.

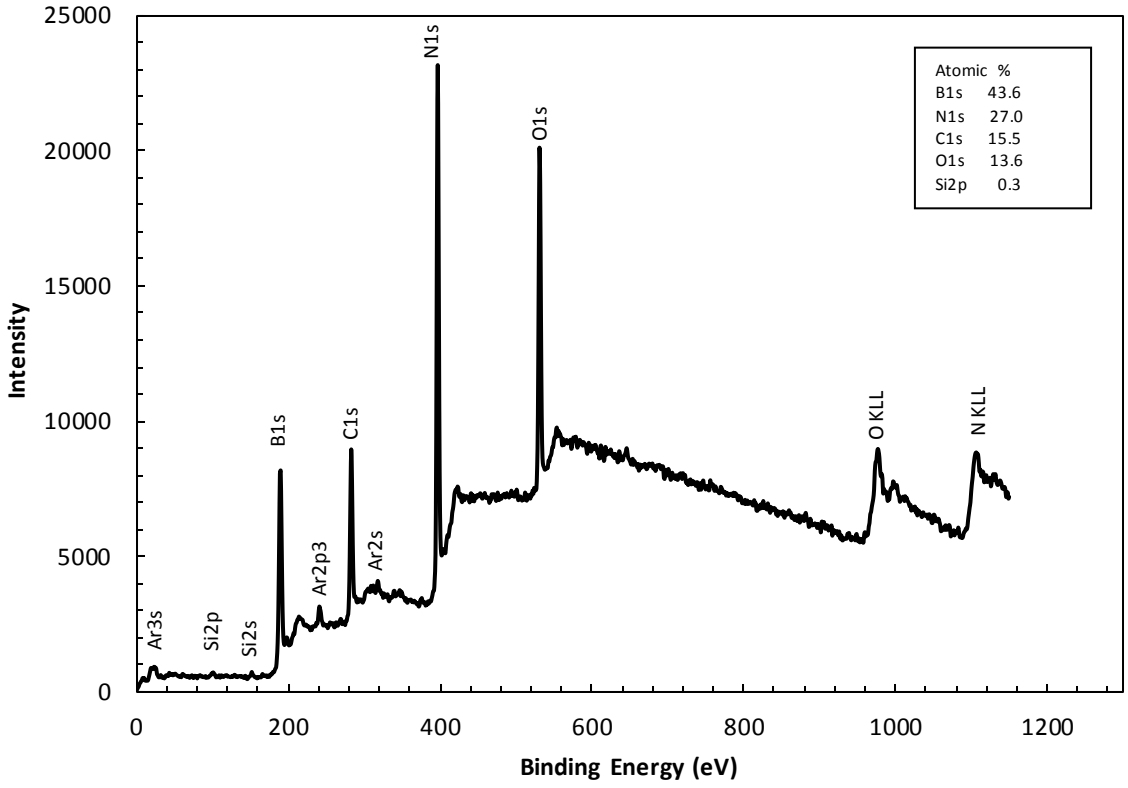

Figure 3.7. XPS analysis of the produced film at 1100^{o}C with atomic percentage (%) of the elements in the product.

XPS analysis of produced boron nitride at 1100^{o}C with the diborane to ammonia molar ratio of 0.050 and total gas flow rate of 150 ml/min gives its major peaks at around 190 eV (B 1s), 283 eV (C 1s), 397 eV (N 1s), 531 eV (O 1s). Peaks at 190.2 eV and 398.2 eV represent presence of boron nitride in the synthesized material [45]. Atomic percentage of O, B and N are 13.6, 43.6, and 27 respectively. The sample was sputtered with argon gas so argon (Ar) element may come from the sputtering process. There is oxygen element in the product which comes from water molecules. The sample was analyzed with carbon layer to provide conductivity so the only source for carbon (C) element is the layer used in the analysis. Silicon (Si) can be accepted as impurity.

The atomic ratio of the elements can be determined using XPS analysis. In this sample, the atomic ratio of boron to nitrogen is not equal to 1.0. If it is equal to 1.0, it would be claimed that the only component in the film is BN. However; the atomic ratio is approximately equal to 1.6. It shows that there are other boron compounds like amorph boron or B_xN_y (x>y) in the produced film. This information can be supported with XRD patterns of the produced boron nitride which have broad diffraction at around 25.5^o.

3.4 Scanning Electron Microscope Analysis of the Film

3.4.1 Effects of Temperature on the Morphology of the Film

In order to observe the effects of different temperatures on the film morphology, four samples produced at different temperatures of 900^oC, 1000^oC, 1100^oC and 1200^oC were selected. The molar ratio of diborane to ammonia was constant at 0.050 and total gas flow rate was 150 ml/min for each of the experiments.

SEM image of boron nitride produced at 900^oC exhibits rough surface morphology (Figure 3.8). In order to make the image of the topography clear, the voltage was increased and it caused cracks on the surface.

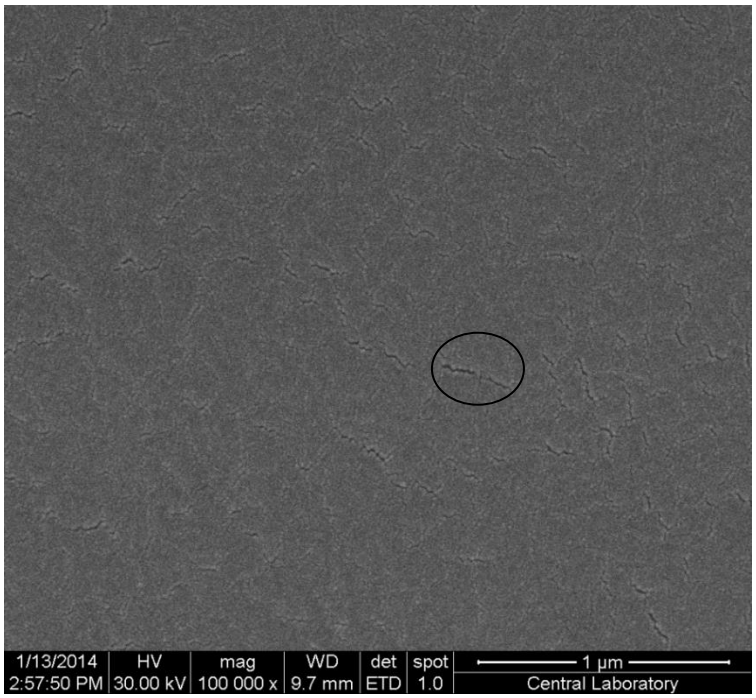

Figure 3.8. SEM image of deposited film produced at 900^{o}C with total flow rate of 150 ml/min and at molar ratio ([B_2H_6]/ [NH_3]) of 0.050.

As it is seen in Figure 3.9, the grain morphology of boron nitride produced at 1000^{o}C is plate-like. Compared with the surface of boron nitride produced at 900^{o}C (Figure 3.8) there is a huge difference in terms of smoothness (or roughness). That means temperature affects the morphology of the produced film.

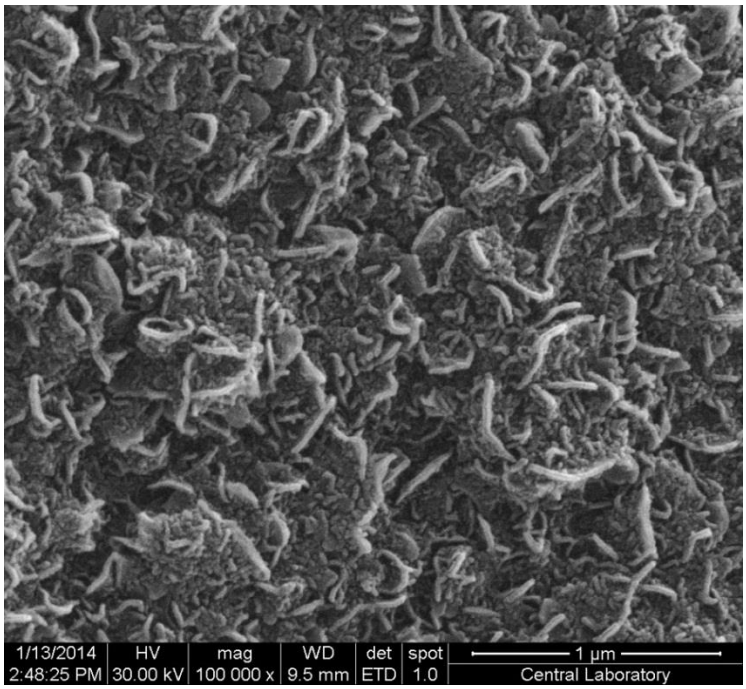

Figure 3.9. SEM image of film produced at 1000^{o}C with total flow rate of 150 ml/min and at molar ratio ([B_2H_6]/ [NH_3]) of 0.050.

According to Figure 3.10, SEM image of film produced at 1100^{o}C also exhibits different morphology compared with that of boron nitride produced at 900^{o}C and 1000^{o}C. Surface morphology of the film is like cauliflower in this case. Plate-like topography at 1000^{o}C changes to rounded grains at 1100^{o}C.

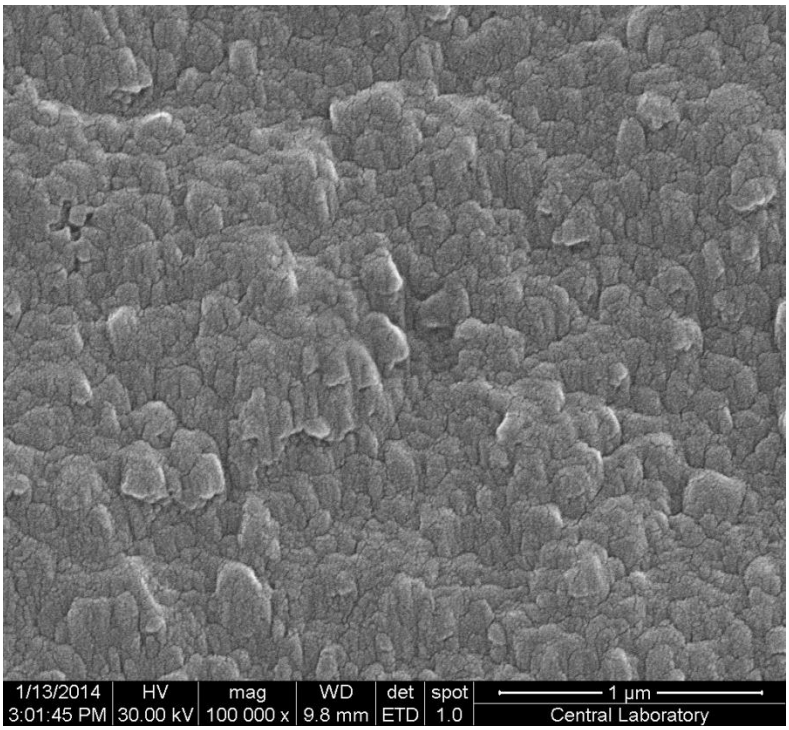

Figure 3.10. SEM image of film produced at 1100°C with total rate of 150 ml/min and at molar ratio ($[B_2H_6]/[NH_3]$) of 0.050.

Surface morphology of deposited film produced at 1200°C is different than the surfaces produced at lower temperatures as seen in Figure 3.11. It is rough and has more fluffy-like topography.

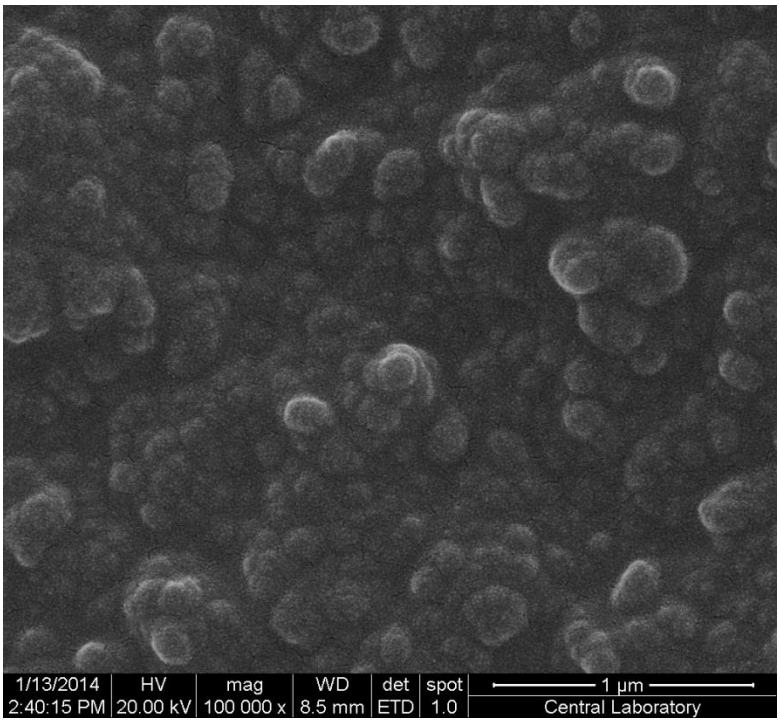

Figure 3.11. SEM image of deposited film produced at 1200^{o}C with total flow rate of 150 ml/min and at molar ratio ($[B_2H_6]/[NH_3]$) of 0.050.

3.4.2 Effects of Molar Ratio of Diborane to Ammonia on the Morphology of the Film

In order to observe the effects of molar ratio of diborane to ammonia on the film morphology, three samples produced at different molar ratio of 0.033 and 0.050 and 0.099 were selected. The temperature was constant at 1100^{o}C and total gas flow rate was 150 ml/min for each of the experiments.

The morphology of the films is pebble-like grains for both of the samples and the topography is rough. It can be claimed that morphology of the films show similar topography at the molar ratio of 0.033 and 0.099 (Figures 3.12 & 3.13).

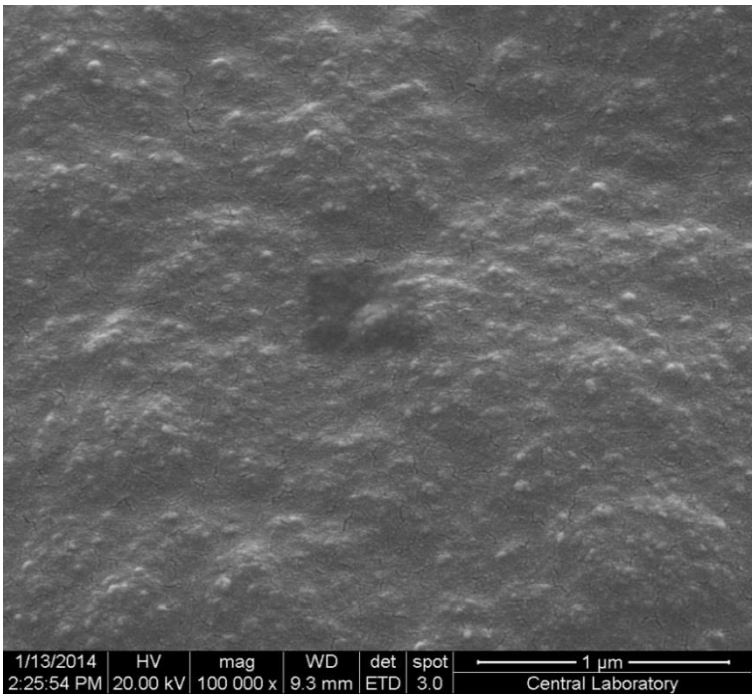

Figure 3.12. SEM image of deposited film produced at 1100°C with total flow rate of 150 ml/min and at molar ratio ($[B_2H_6]/[NH_3]$) of 0.099

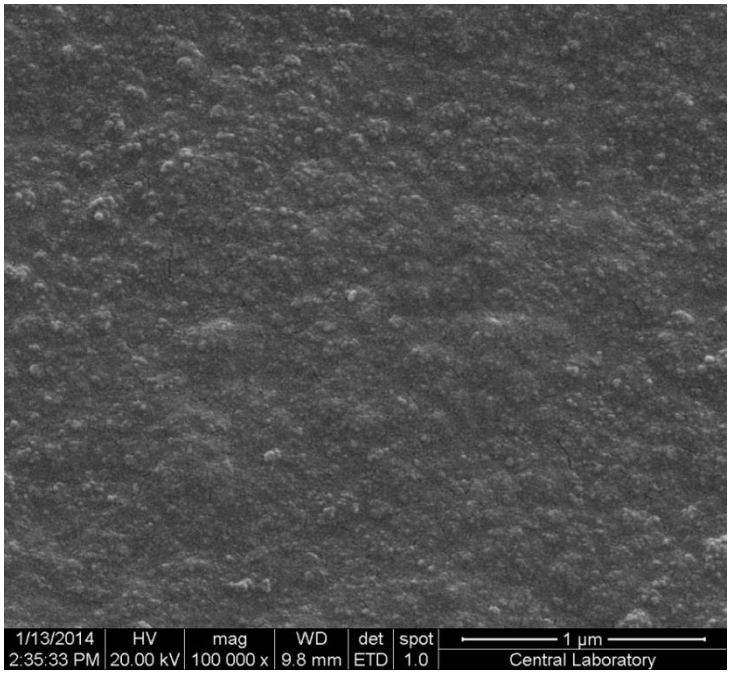

Figure 3.13. SEM image of deposited film produced at 1100°C with the total flow rate of 150 ml/min and at molar ratio ($[B_2H_6]/[NH_3]$) of 0.033.

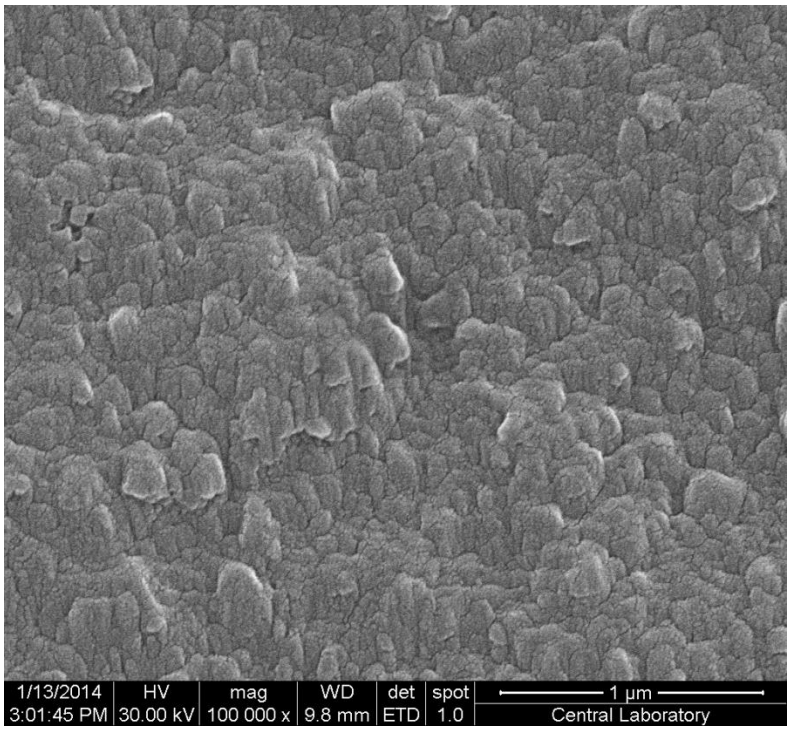

Figure 3.14. SEM image of film produced at 1100^{o}C with a molar ratio ([B_2H_6]/ [NH_3]) of 0.050.

As seen in Figure 3.14, the SEM image of film produced at the molar ratio of 0.050 shows different topography compared with other two SEM images (Figure 3.12 and Figure 3.13). It has rough surface and rounded grains at 1100^{o}C. It may imply that molar ratio of 0.050 affects the morphology of the film.

3.5 Deposition Rate of the Film at Different Temperatures

Total 23 experiments were conducted to collect information about how reaction temperature affects the deposition rate of the film (Appendix D.3). In order to calculate deposition rate, weight of the substrate was measured before and after the experiments. Weights of the substrates for different experimental conditions are tabulated in Tables D.3.1, D.4.1 and D.5.1 in Appendix D. Deposition rate of the film (R_F) can be calculated using Equation (3.5.1) where w_f is the final weight of the film after each of

the experiments w_i ,initial weight, is measured with precision scale before placing the foil in the reactor and Δt is the reaction time.

$$R_F = \frac{W_f - W_i}{\Delta t} \quad (3.5.1)$$

After the experiments, it was observed that the color of the produced films is different from each other. It is close to transparent at 900°C to 1000°C and it is clearly transparent at 1100°C and white at 1200°C. It can explain the differences on the surface morphology of the samples in SEM images.

Each experiment was repeated more than 3 times except the one at 900°C so in order to obtain consistent experimental error, three of them were taken into standard deviation calculation (Appendix D.1) for each set. As a result, as seen in Figure 3.15, it is found that deposition rate is positively correlated with temperature. More explicitly, growth rate of boron nitride (BN) on tungsten substrate increases with the temperature increase.

At temperatures lower than 900°C, it was observed that, there is no deposition on the surface. The experiments conducted at the temperatures higher than 1200°C did not provide credible data to analyze. Therefore, the temperature range was selected between 900°C and 1200°C.

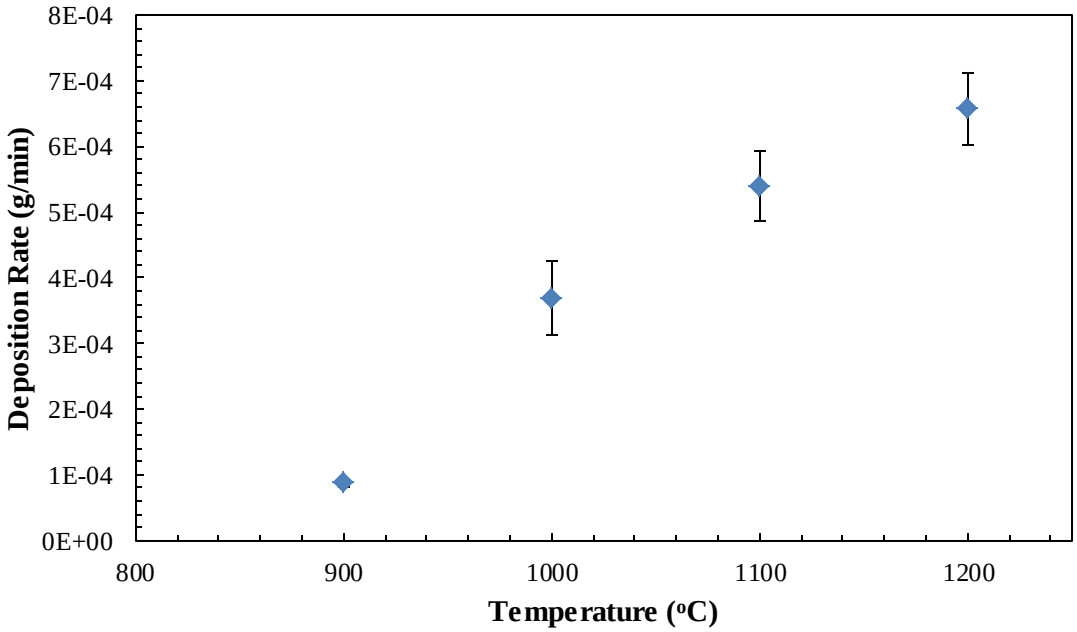

Figure 3.15. Change in deposition rate of the film on tungsten substrate depending on temperature (Total flow rate: 150 ml/min and molar ratio of $[B_2H_6]/[NH_3]$: 0.050.)

3.6 Deposition Rate at Different Molar Ratios ($[B_2H_6]/[NH_3]$)

In the molar ratio experiments, the diborane flow rate was kept constant and ammonia flow rate was changed to observe the effect of the molar ratio of the reactants on the deposition rate. In these experiments molar ratio was studied at values of 0.099, 0.050 and 0.033. As it is seen in the Figure 3.16 when the flow rate of the ammonia increases, the molar ratio decreases although there is a small increase in the molar ratio of 0.050. After the experiments it was observed that the deposition rate at molar ratio of 0.033 was slightly less than that at the molar ratio of 0.050, however; both is in the range of standard deviation so they can be accepted as the same. This situation might be explained with the possible side reactions, which suppress the main reaction between diborane and ammonia. XPS analysis supports the possible side reactions by giving

different atomic ratios of B to N and XRD analyses also show that broad peaks around 25.5^{o} might come from other boron compounds.

If there are no side reactions, the only reaction should be;

$$B_2H_6 + 2NH_3 \rightarrow 2BN + 6H_2$$

However, possibly there are gas phase reactions (B_2H_6 is very reactive and NH_3 decomposes in the gas phase [45]) and other reactions on the surface, which complicate the picture. More data on the gas phase analysis and mechanism of the reactions are needed to have a clear understanding of how deposition rate changes with molar ratio.

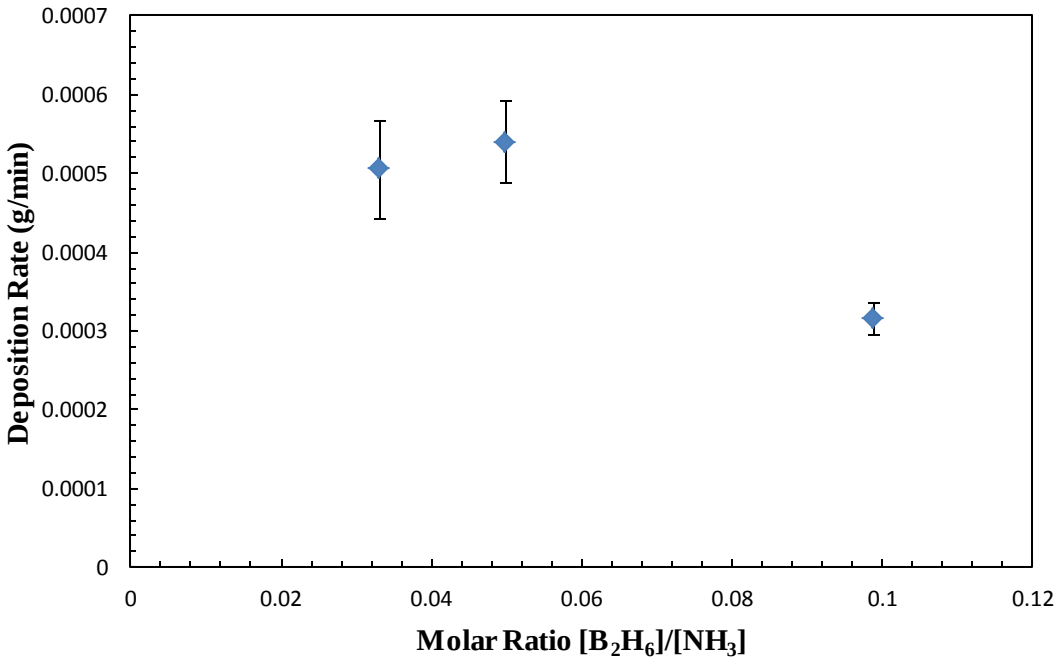

Figure 3.16. Change in deposition rate of the film on tungsten substrate depending on molar ratio of ([B_2H_6]/[NH_3]). (Total flow rate: 150 ml/min and the substrate temperature, T_s: 1100^{o}C)

3.7 Deposition Rate at Different Total Flow Rates

In order to analyze how total flow rate affects the deposition rate, the molar ratio of $[B_2H_6]/[NH_3]$ was kept constant at 0.050 for each flow rate and experiments were conducted under the same temperature of 1000°C.

In this case, it is observed that (Figure 3.17) when the total flow rate increases, from 100 ml/min to 125 ml/min, deposition rate increases. However; when total flow rate increases to 150 ml/min and 175 ml/min, deposition rate decreases. That behavior may be explained by considering the possible decrease of mass transfer resistance by increase of impingement on the substrate with the increase of flow rate. However; at higher flow rates residence time of reactants decrease which results in decrease of deposition rate.

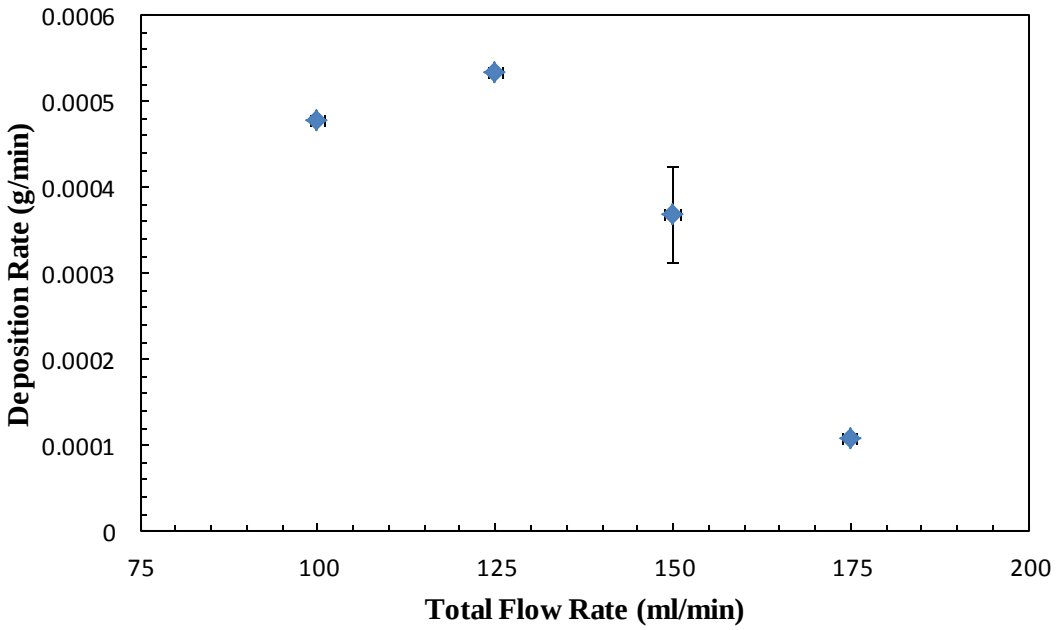

Figure 3.17. Deposition rate of the film on tungsten substrate for different total flow rates. (Molar ratio $[B_2H_6]/[NH_3]$: 0.050 and substrate temperature T_s: 1000°C).

3.8 Thickness Analysis of Deposited Film at Different Temperatures and Molar Ratios ($[B_2H_6]/[NH_3]$)

Thickness analysis of deposited film was done using digital caliper. The length of each substrate is 1.2 cm and the width of the substrate is 2.5 mm. Five points vertically were determined along the film to measure the thicknesses.

It is found that the average film thicknesses are 0.395 mm, 0.745 mm, 1.135 mm and 1.395 mm at the temperatures of 900^{o}C, 1000^{o}C, 1100^{o}C, and 1200^{o}C respectively. It can be claimed that thickness of the films increase with temperature.

The thicknesses of the deposited film produced at different temperatures can be seen in Figure 3.18. As it is mentioned before, the maximum thickness of the film is observed in the middle of the film where the mass transfer resistance is almost zero due to impingement of the reactants on the surface. The distribution of the deposited BN on the film is symmetrical on both sides.

The numbers on Figure 3.18 and Figure 3.19 represent the thickest points on the film which are calculated from thickness of the film after subtracting the substrate's (tungsten foil) thickness of 0.025 mm. The data collected from the film for thickness analyses are tabulated in Appendix E.

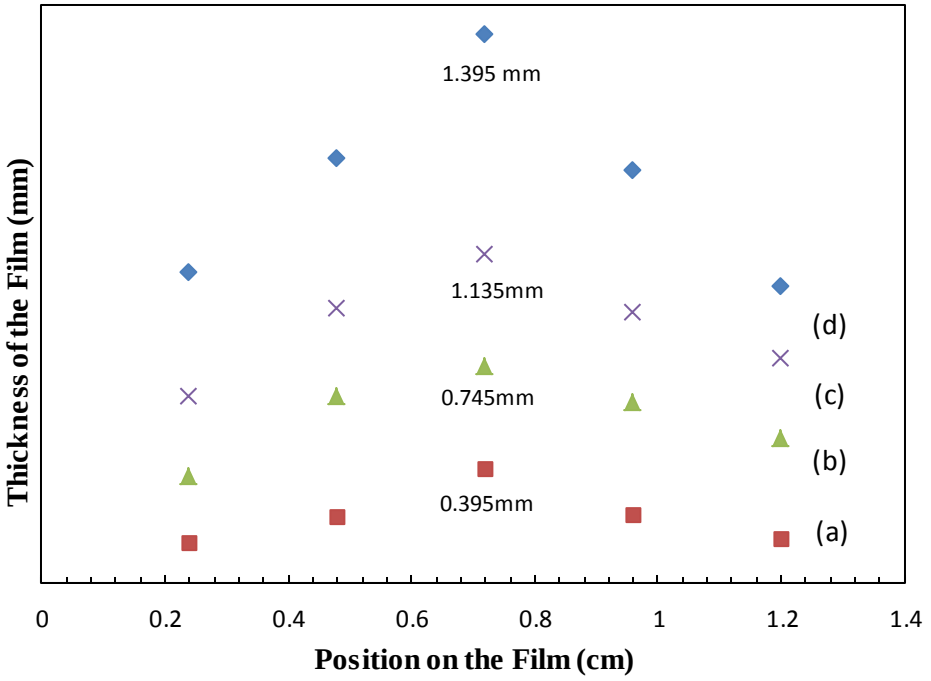

Figure 3.18. Thickness of the deposited film produced at different temperatures (a) 900°C, (b) 1000°C, (c) 1100°C and (d) 1200°C with total flow rate of 150 ml/min and at molar ratio $[B_2H_6]/[NH_3]$ of 0.050.

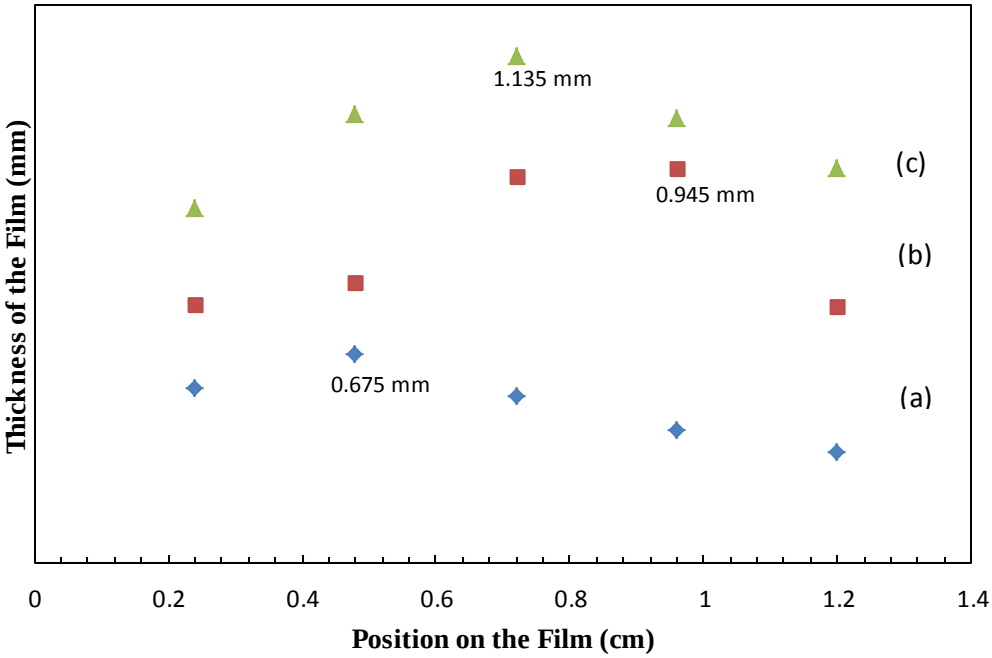

Figure 3.19. Thickness of the deposited film produced at different molar ratios $[B_2H_6]/[NH_3]$ of (a) 0.099, (b) 0.033, (c) 0.050 with total flow rate of 150 ml/min and substrate temperature is 1100^oC

The change in the thicknesses of the deposited film produced with molar ratios $[B_2H_6]/[NH_3]$ can be seen in Figure 3.19. It is found that at molar ratio $[B_2H_6]/[NH_3]$ of 0.050, thickness of the film is maximum. It is expected to achieve maximum thickness in the middle of the surface, however; in some cases the substrate may deviate from the center due to the position of the film in the reactor. After subtracting the thickness of the substrate from the total thickness of film measured, it is found that the average film thicknesses are 0.675 mm, 0.945 mm, 1.135 mm at the molar ratios $[B_2H_6]/[NH_3]$ of 0.099, 0.033 and 0.050, respectively.

CHAPTER 4

CONCLUSIONS AND RECOMMENDATIONS

Boron nitride (BN) production on tungsten substrate in impinging jet reactor was achieved using CVD method. XRD, XPS, Raman Spectroscopy and SEM analysis were used to collect information about the crystalline structure and morphology of the product. At the temperatures lower than 900^{o}C, h-BN cannot be deposited.

All the analyses show that hexagonal boron nitride is successfully produced on tungsten substrate using the CVD method. The effects of different parameters on deposition rate like temperature, molar ratio and total flow rate were examined.

XRD analyses for different reaction temperatures show that crystallinity of boron nitride increases when the temperature increases and the deposit contains h-BN together with other compounds.

Deposition rate is almost constant at molar ratio values less than 0.050 but the rate decreases at higher molar ratio values. Deposition rate increases with substrate temperature. Moreover, the deposited film changes from transparent to white as the temperature increases.

Raman spectroscopy is assumed as the fingerprints of the molecules. Our Raman and XPS spectra clearly show that the deposits obtained contain h-BN.

In our experimental set-up, the highest deposition rate was obtained at 1200^{o}C with a total flow rate of 150 ml/min and molar ratio $[B_2H_6]/[NH_3]$ of 0.050. Deposition rate measurements show the decrease of deposition rate with high molar ratio of $[B_2H_6]/[NH_3]$. That may imply the decrease of reaction rate with high molar ratio,

however; this must be verified with gas phase analyses, and that could be subject of a future study.

At higher temperatures such as 1300^{o}C cubic boron nitride formation might be observed. Therefore, the system must be arranged to achieve deposition at higher temperatures.

REFERENCES

[1] R.T. Paine, C.K. Narula, "Synthetic Routes to Boron Nitride" *Chem. Rev.*, **90**(1990), 73-91.

[2] SubsTech, Substances and Technologies, www.substech.com/dokuwiki/doku.php?id=boron_nitride_as_solid_lubricant, last visited on August 2013

[3] Li S., Zhang L., Ye F., Cheng L., Feng Z., and Chen L., "Effect of temperature on the microstructure of boron nitride formed in situ on chemical vapor deposited boron in ammonia gas" *J. Am. Ceram. Soc.* **94**(2011) 3.

[4] John J. Pounch, S.A. Alterovitz, 'Synthesis and Properties of Boron Nitride', Vol. 54&55, Trans Tech Publications, USA, 1990.

[5] Pierson H.O, Handbook of Chemical Vapor Deposition; Noyes Publications, New York, 1999.

[6] A.C Jones, M.L. Hitchman, Chemical Vapor Deposition: Precursors, Processes and Applications; RSC Publishing, Cambridge, 2009

[7] Y.Cheng, X. Yin, Y. Liu, S. Li, L. Cheng, L. Zhang, "BN coatings prepared by low pressure chemical vapor deposition using boron trichloride-ammonia-hydrogen-argon mixture gases" *Surface and Coatings Technology*, **204** (2010) 2797-2802.

[8] Sherman A., 'Chemical Vapor Deposition for Microelectronics, Principles, Technology and Applications', Noyes Publication, New Jersey, USA, 1987

[9] Connexions, http://cnx.org/content/m25495/latest/, last visited on August 2013

[10]IEEExplore,Digital,Library,http://xplqa30.ieee.org/xpls/icp.jsp?arnumber=5966348, last visited on August 2013

[11] Galerie A., 'Vapor Surface Treatments'; Wiley Publication, USA, 2010.

[12] Oxford Instruments, www.oxford-instruments.com/deposition –processes last visited on June 2011

[13] A. Kar, J. Mazumder, 'Laser Processing: Surface Treatment and Film Deposition', Volume 307, Springers Netherlands, 1996 pp 203-235

[14] LMNF Laboratory, http://laser.gist.ac.kr/board/bbs/board.php?bo_table=rese_02 last visited on August 2013

[15] J. Park, T.S. Sudarshan, 'Chemical Vapor Deposition', Volume 2, ASM International, July 2001 pp 380

[16] Laboratório Associado de Plasma – LAP, http:// www. plasma. inpe.br /LAP _Portal/LAP_Site/Text/Plasma_Processing.htm, last visited on August 2013

[17] Wikipedia, https://en.wikipedia.org/wiki/Metalorganic_vapour_phase_epitaxy last visited on July 2013

[18] C.G. Aleixandre, D. Diaz, F. Orgaz and J.M., Albella, "Reaction of diborane and ammonia gas mixtures in a chemical vapor deposition hot wall reactor" *J.Phys.Chem.*, **97** (1993), 11043-11046

[19] J.Li, C. Zhang, B. Lin, F. Cao, S. Wang, "Boron nitride Coatings by chemical vapor deposition from borazine" *Surface and Coatings Technology*, **205** (2011) 3736-3741

[20] C.G. Aleixandre, A. Essafti, M. Fernandez, J.L.G. Fierro, and J.M. Albella, "Influence of diborane flow rate on the structure and stability of boron nitride films" *J. Phys. Chem*., **100** (1995), 2148-2153

[21] Y. Jin, S.Lee, Y. Nam, J.K.Lee and D. Park, "A study of deposition rate and characterization of BN thin films prepared by CVD", *Korean J. Chem. Eng.*, **15**(6) (1998) 652-657

[22] T. Usamia, T.Asaji, S. Matsumoto, H. Kanda, K. Nakamura, "Deposition of BN films on metal substrates from a fluorine containing plasma" *Surface & Coatings Technology,* **203** (2009) 929-933

[23] J.L. Andujar, E. Bertran, M.C. Polo, "Plasma-enhanced chemical vapor deposition of boron nitride thin films from B_2H_6-H_2-NH_3 and B_2H_6-N_2 gas mixtures", *J. Vac. Sci. Technol. ,* **A16(2)** (1998) 578-586

[24] D. Franz, M. Hollenstein, Ch. Hollenstein, "Diborane nitrogen/ammonia plasma chemistry investigated by infrared absorption spectroscopy" *Thin Solid Films,* **379** (2000) 37-44

[25] B. Choi, "Chemical vapor deposition of hexagonal boron nitride films in the reduced pressure" *Materials Research Bulletin,* **34** (1999) 2215-2220

[26] Y. Ye, U. Graupner, R. Kruger, "Hexagonal boron nitride from a borazine precursor for coating of SiBNC fibers using continuous atmospheric pressure CVD process" *Chem. Vap. Deposition*, **17** (2011) 221-227

[27] Frueh S., Kellett R., Mallery C., Molter T., Willis W.S., King'ondu C. and Suib S.L., "Pyrolytic decomposition of ammonia borane to boron nitride" *Inorg. Chem.* **50**(2011) 783-792

[28] Dalui S., Pal A.K., "Microstructural and optical properties of BN films deposited by inductively coupled plasma CVD", *Vacuum* **82**(2008) 1296-1301

[29] Gafri O., Grill A. and Itzhak D., "Boron nitride coatings of steel and graphite produced at a low pressure r.f. plasma" *Thin Solid Films,* **72**(1980) 523-527

[30] Zheng Y., Wang S., "Synthesis of boron nitride coatings on quartz fibers: thickness control and mechanism research" *Applied Surface Science* **257**(2011) 10752-10757

[31] Li J., Zhang C. and Li B., "Preparation and characterization of boron nitride coatings on carbon fibers from borazine by chemical vapor deposition" *Applied Surface Science* **257**(2011) 7752-7757

[32] Yuan S., Zhu L., Fan M., Wang X., Wan D., Peng S., Tang H., " Fluffy-like boron nitride spheres synthesized by epitaxial growth" *Material Chemistry and Physics*, **112**(2008) 912-915

[33] Karaman M., Sezgi N.A., and Özbelge H. *Ö.*, "Production of B_4C coatings by CVD method in a dual impinging-jet reactor: chemical yield, morphology and hardness analysis", *AlChE J.*, **55**(2009), 2914-2919

[34] Sezgi N.A., Ersoy A.,*Doğu* T., Özbelge H.*Ö.*, "CVD of boron and dichloroborane formation in a hot-wire fiber growth reactor" *Chemical Engineering and Processing* , **40**(2001) 525-530

[35] Sezgi N.A.,*Doğu T.,Özbelge* H.*Ö.*, "Mechanism of CVD of boron by hydrogen reduction of BCl_3 in a dual impinging-jet reactor" *Chemical Engineering Science*, **54**(1999) 3297-3304

[36] Dilek S.N., *Özbelge* H. *Ö.*, Sezgi N.A.,Doğu *T.*, "Kinetic studies for boron carbide formation in a dual impinging-jet reactor", *Ind.Eng. Chem.Res.* ***40****(2001), 751-755*

[37] Sezgi N.A., *Doğu T.,* Özbelge H. *Ö.*, "$BHCl_2$ formation during chemical vapor deposition of boron in a dual-impinging jet reactor" *Ind. Eng. Chem. Res.*, **36**(1997) 5537-5540

[38] College of Engineering and Mineral Resources, www2.cemr.wvu.edu/~wu/mae649/xps.pdf, last visited on August 2013

[39] Documents and Resources for Small Businesses and Professionals, http://www.docstc.com/docs/12282407/4-XPS-or-ESCA-2009-revised-B, last visited on August 2013

[40] Online Book, http://fds.oup.com/www.oup.com/pdf/13/9780199219667.pdf , last visited on August 2013

[41] MIT, http://pruffle.mit.edu/atomiccontrol/education/xray/xray_diff.php, last visited on August 2013

[42] Geochemical Instrumentation and Analysis, http://serc.carleton.edu/research_education/geochemsheets/techniques/SEM.html, last visited on August 2013

[43] Purdue University, http://www.purdue.edu/rem/rs/sem.htm, last visited on August 201

[44] Frost R.L., Bahfenne S. 'Infrared and infrared emission spectroscopic study of selected magnesium carbonate minerals artinite and dypingite' p.8

[45] Özmen D., Sezgi N.A., Balci S., "Synthesis of boron nitride nanotubes from ammonia and a powder mixture of boron and iron oxide", *Chemical Engineering Journal* **219**(2013) 28-36

[46] Andor Technology, http://www.andor.com/learning-academy/raman-spectroscopy-an-introduction-to-raman-spectroscopy, last visited on January 2014

APPENDIX A

CALIBRATION CURVES FOR ARGON AND AMMONIA MASS FLOW CONTROLLER

A.1 Calibration Curve for Argon Mass Flow Controller

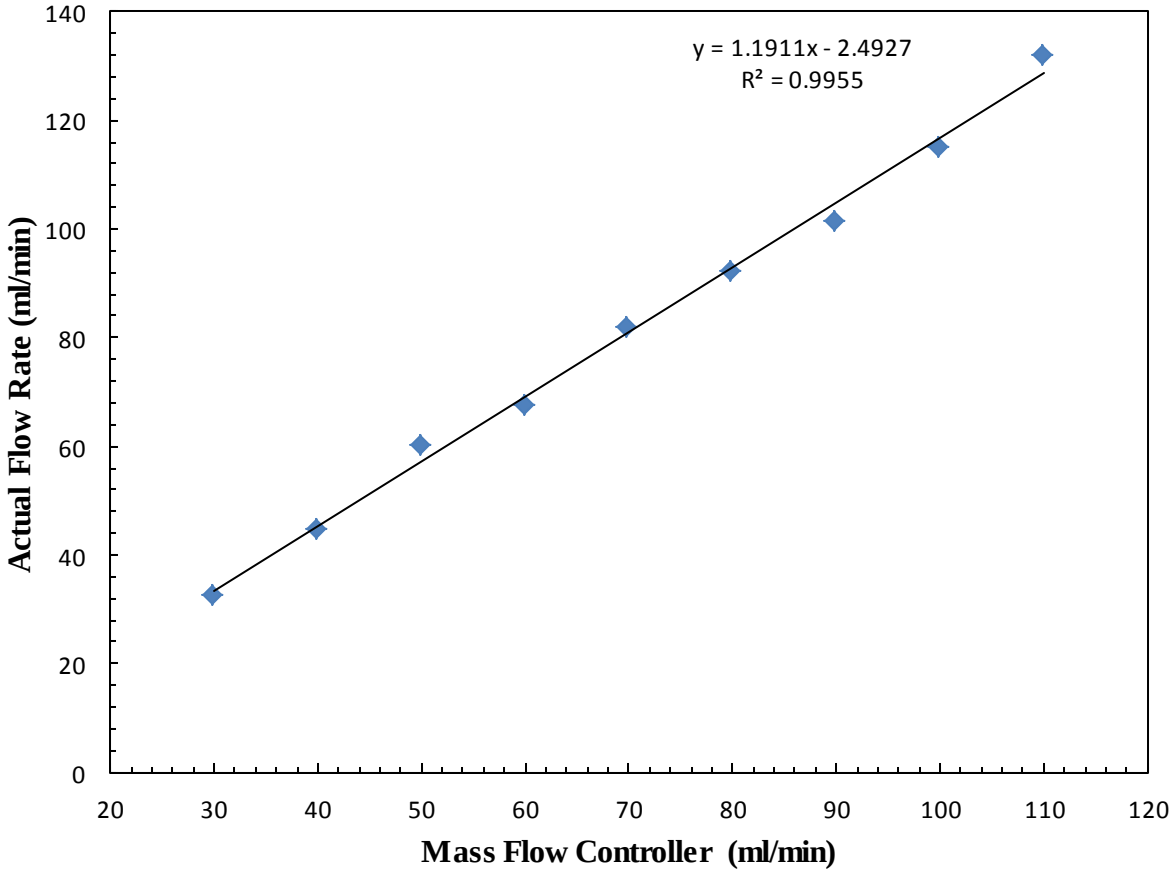

Figure A.1: Volumetric flow rate calibration curve for argon mass flow controller

A.2 Calibration Curve for Ammonia Mass Flow Controller

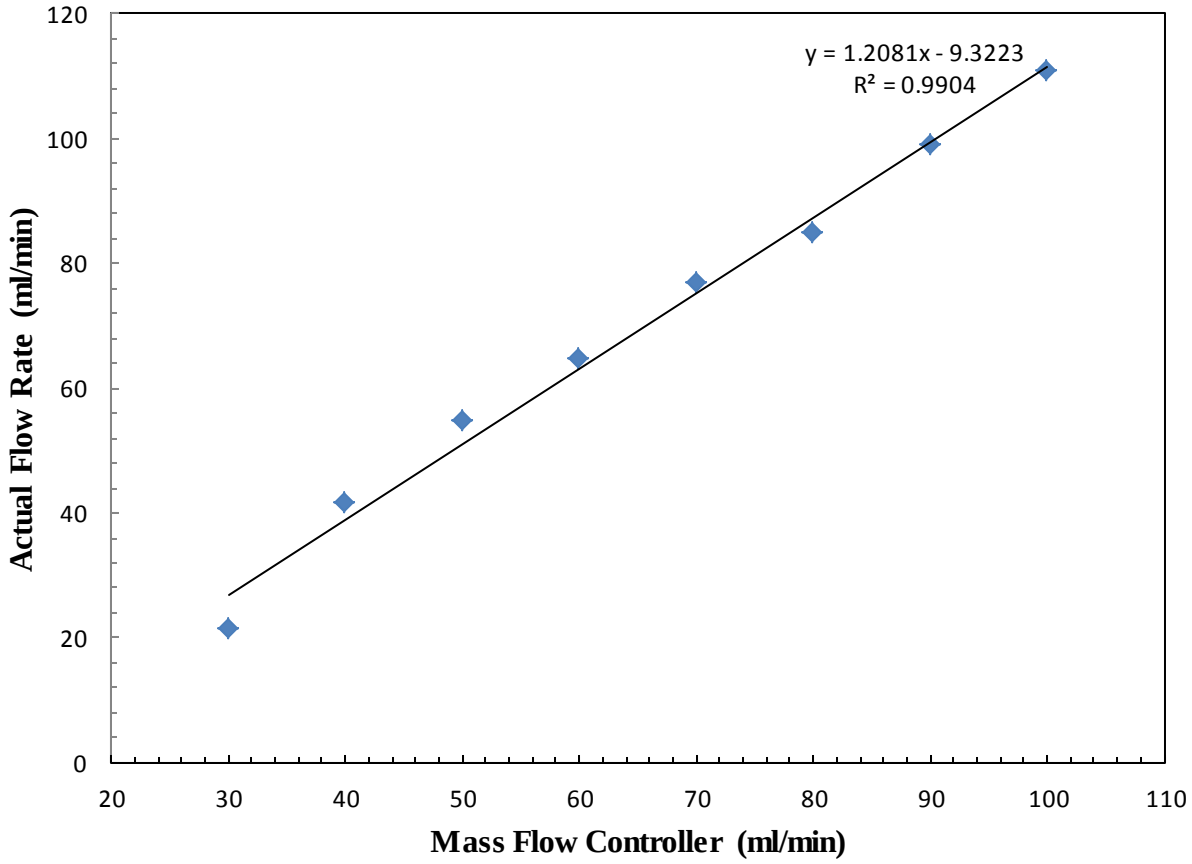

Figure A.2 : Volumetric flow rate calibration curve for ammonia mass flow controller

APPENDIX B

CALCULATION OF B_2H_6 MOLAR RATIO

Diborane gas mixture includes 10% of B_2H_6 and 90% of NH_3 , ammonia gas mixture includes 99.999% NH_3 so it can be assumed as pure ammonia. The surface reaction is assumed as to be

$$B_2H_6 + 2NH_3 \leftrightarrow 2BN + 6H_2$$

Volumetric flow rate of diborane gas mixture is 15ml/min and volumetric flow rate of ammonia (NH_3) is 30ml/min when total flow rate is 150 ml/min. Diborane (B_2H_6) is 10% vol in the gas mixture so the volumetric flow rate of B_2H_6 is 1.5 ml/min. If the gas mixtures are assumed as ideal gas then molar ratio of B_2H_6/ NH_3 is found as 0.050. The same result can be obtained using density of the gases. Densities of B_2H_6, NH_3 were the values at 1.013 bar and 15°C.

$\dot{M} = \rho * Q$

where ρ is density, Q is volumetric flow rate and $\dot{M}$ is mass flow rate of gases

$n_{B2H6/} n_{NH3=} (6.39x10^{-5}mol/min)/(1.285x10^{-3}mol/min)=0.0497=\sim 0.050$

Table B 1: Physical Properties and Flow Rate Values of Ammonia and Diborane

	Density, ρ (kg/m^3)	Molecular Weight (g/mol)	Volumetric Flow Rate, Q (m^3/min)	Mass Flow Rate, $\dot{M}$ (g/min)	Molar Flow Rate (mol/min)
Ammonia	0.73	17.03	$30*10^{-6}$	$2.19*10^{-3}$	$1.285*10^{-3}$
Diborane	1.18	27.67	$15*10^{-6}$	$1.77*10^{-3}$	$6.39*10^{-5}$

APPENDIX C

X-RAY DIFFRACTION DATA

C.1 X-Ray Diffraction Data for Hexagonal Boron Nitride

Table C.1 1: XRD Data of h-BN (34-0421)

Catalog No: 34-0421 Hexagonal BN Rad:CuKa1 (λ:1.5406)					
d	2θ	Int	h	k	l
3.328	26.76	100	0	0	2
2.169	41.59	23	1	0	0
2.062	43.87	10	1	0	1
1.817	50.14	16	1	0	2
1.663	55.16	12	0	0	4
1.550	59.55	<2	1	0	3
1.319	71.41	5	1	0	4
1.252	75.93	13	1	1	0
1.172	82.17	14	1	1	2
1.134	85.51	<3	1	0	5
1.109	87.94	<3	0	0	6
1.084	90.53	<3	2	0	0
1.031	96.66	3	2	0	2
1.000	100.68	10	1	1	4
0.987	102.49	<3	1	0	6

Table C.1 2: XRD Data of h-BN (45-0893)

Catalog No: 45-0893 Hexagonal BN Rad:CuKa1 (λ:1.5406)					
d	2θ	Int	h	k	l
3.33	26.74	100	0	0	2
2.17	41.58	26	1	0	0
1.820	43.69	10	1	0	1
1.670	50.07	27	1	0	2
1.320	54.93	12	0	0	4
1.250	59.59	2	1	0	3
3.330	71.4	8	1	0	4
2.170	76.08	19	1	1	0

Table C.1 3: XRD Data of h-BN (45-0895)

Catalog No: 45-0895 Hexagonal BN Rad:CuKa1 (λ:1.5406)					
d	2θ	Int	h	k	l
3.330	26.74	100	0	0	2
2.170	41.58	11	1	0	0
2.070	43.69	37	1	0	1
1.820	50.07	11	1	0	2
1.670	54.93	12	0	0	4
1.550	59.59	11	1	0	3
1.320	71.4	3	1	0	4
1.250	76.08	5	1	1	0

Table C.1 4: XRD Data of h-BN (45-0893)

Catalog No: 45-0893 Hexagonal BN Rad:CuKa1 (λ:1.5406)					
d	2θ	Int	h	k	l
3.330	26.74	100	0	0	2
2.170	41.58	32	1	0	0
1.820	50.07	33	1	0	2
1.670	54.93	12	0	0	4
1.320	71.4	8	1	0	4
1.250	76.08	19	1	1	0

Table C.1 5: XRD Data of Tungsten

Tungsten (W) Rad:CuKa1 (λ:1.5405)		
d	2θ	Int
2.238	40.26	100
1.292	73.19	23
0.8459	131.17	18
1.582	58.27	15
1.0008	100.64	11
1.1188	87.02	8
0.9137	114.92	4
0.7912	153.57	2

APPENDIX D

DEPOSITION RATE DATA

D.1 Deposition Rate Data at Different Temperatures

Calculation of standard deviation is done according to the equation below,

$$s = \sqrt{\frac{\sum(x - \bar{x})^2}{N - 1}}$$

s = the standard deviation

x = weight of deposited film

$\bar{x}$ = the mean of the weights of deposited film produced at the same temperature

N = the number of values (the sample size)

Table D.1 1 Deposition Rate of the Film Produced at Different Temperatures

Temperature(^{o}C)	Weight of Deposited Film (g)	Deposition Rate (g/min)	Std (+/-)
900	0.00523	0.00009	4.81E-06
1000	0.0221	0.000368	5.66E-05
1100	0.0324	0.000539	5.23E-05
1200	0.0284	0.000658	5.43E-05

D.2 Deposition Rate Data at Different Molar Ratios of Diborane to Ammonia

Table D.2 1: Deposition Rate of The Film Produced at Different Molar Ratios of Diborane to Ammonia.

Molar Ratio of [B2H6/NH3]	Deposition Rate (g/min)	Std(+/-)
0.033	0.000505	6.19E-05
0.050	0.000539	5.23E-05
0.099	0.000315	2.12E-05

D.3 Experimental Data for Different Temperatures

Table D.3 1: Raw Data for Experiments Carried out at Different Temperatures

Temperature (^{o}C)	Initial Weight (g)	Final Weight (g)	Deposition Rate (g/min)
900 ∓18.09	0.0281	0.0335	0.000090
	0.0266	0.0315	0.000082
	0.0276	0.033	0.000090
1000 ∓18.79	0.0306	0.0504	0.000330
	0.0314	0.0519	0.000342
	0.0298	0.0558	0.000433
1100 ∓23.24	0.0246	0.0524	0.000463
	0.0274	0.0628	0.000590
	0.0253	0.0590	0.000562
1200 ∓16.31	0.0279	0.063	0.000716
	0.0282	0.0556	0.000609
	0.0265	0.0492	0.000649

D.4 Experimental Data for Different Molar Ratios

Table D.4 1: Data Collected for Experiments at Different Molar Ratios of B_2H_6 to NH_3

Temperature (^oC)	Molar Ratio of B_2H_6 to NH_3	Initial Weight (g)	Final Weight (g)	Deposition Rate (g/min)
1100 ∓17.54	0.033	0.0253	0.0518	0.00044167
		0.0255	0.0484	0.00038167
		0.0257	0.0390	0.00044333
		0.0226	0.0441	0.00035833
		0.0284	0.0559	0.00045833
1100 ∓23.24	0.050	0.0290	0.0634	0.00057333
		0.0246	0.0524	0.00046333
		0.0296	0.0601	0.00050833
		0.0274	0.0628	0.00059000
		0.0253	0.0590	0.00056167
1100 ∓13.41	0.099	0.0285	0.0483	0.00033000
		0.0250	0.0430	0.00030000

D.5 Experimental Data for Different Total Gas Flow Rate

Table D.5 1: Data Collected for Experiments at Different Total Gas Flow Rates

Total Flow Rate (ml/min)	Initial Weight (g)	Final Weight (g)	Deposition Rate (g/min)
100	0.07220	0.09609	0.000478
125	0.07130	0.10060	0.000586
150	0.03060	0.05270	0.000368
175	0.07150	0.07580	0.000108

APPENDIX E

THICKNESS MEASUREMENT DATA

Table E.1: Data Collected for Thickness Analyses at Different Surface Temperatures

Length of the Film (cm)	Thickness (mm)			
	900 ^{o}C	**1000 ^{o}C**	**1100 ^{o}C**	**1200 ^{o}C**
0.24	0.135	0.365	0.645	0.575
0.48	0.225	0.645	0.945	0.965
0.72	0.395	0.745	1.135	1.395
0.96	0.235	0.625	0.935	0.925
1.20	0.155	0.495	0.775	0.525

Table E.2: Data Collected for Thickness Analyses at Different Molar Ratios Diborane to Ammonia

	Thickness (mm)		
Length of the Film (cm)	Molar Ratio of **0.033**	Molar Ratio of **0.050**	Molar Ratio of **0.099**
0.24	0.535	0.645	0.565
0.48	0.605	0.945	0.675
0.72	0.945	1.135	0.535
0.96	0.975	0.935	0.425
1.2	0.525	0.775	0.355

APPENDIX F

XRD PATTERN OF TUNGSTEN SUBSTRATE

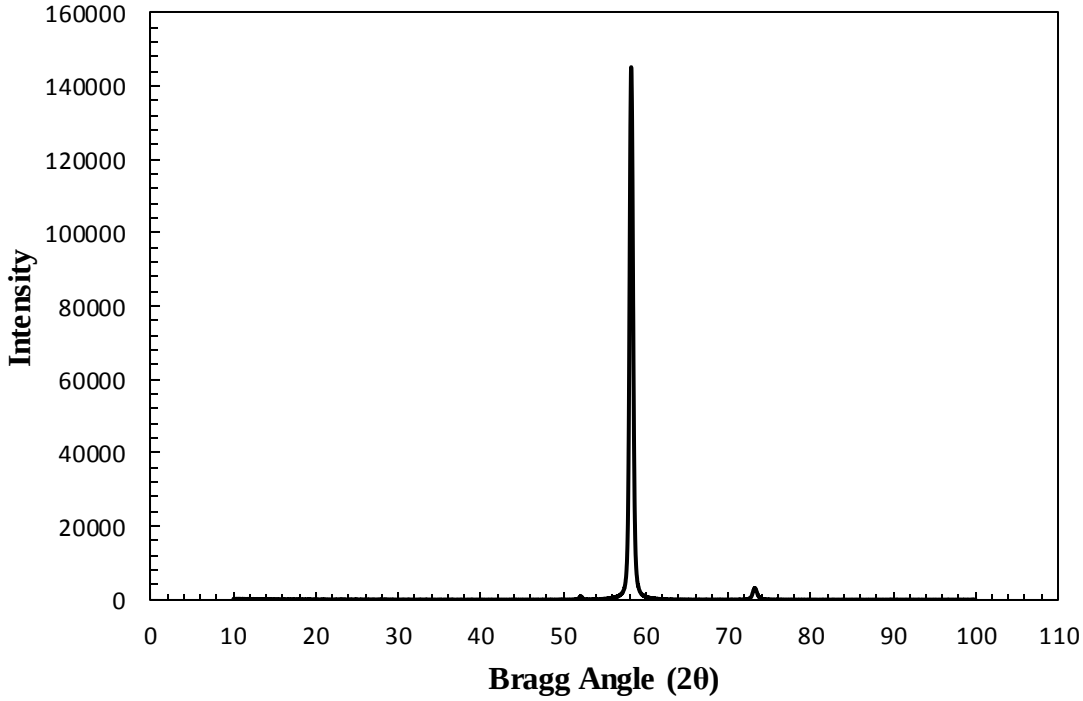

Figure F.1. XRD pattern of Tungsten (W) Substrate